ECG BASED AUTOMATIC DIAGNOSIS AND LOCALIZATION OF MYOCARDIAL INFARCTION

INITIAL THESIS DARFT

By

IJAZ AHMAD (BS-CIS 2005-2009)
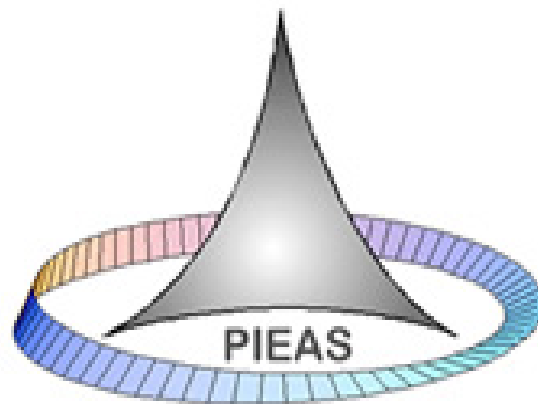
PROJECT SUPERVISORS

DR. M. ARIF

MR. FAYYAZ UL AMIR AFSAR MINHAS

Department of Computer and Information Sciences

Pakistan Institute of Engineering and Applied Sciences

Nilore-45650, Islamabad

April 20, 2009

CERTIFICATE OF APPROVAL

This is to certify that the thesis work entitled:

"ECG BASED AUTOMATIC DIAGNOSIS AND LOCALIZATION OF MYOCARDIAL INFARCTION"

Was carried out by:

MR. IJAZ AHMAD

Is approved for submission to the panel by:

Signature: _____

MR. FAYYAZ UL AMIR AFSAR MINHAS

DCIS PIEAS

To

The loving memory of my Father,

My loving Mother,

My dear and loving sister Sumaira,

My Great brother M. Iskhaq,

And all my teachers especially Mr. Shukat Hussain,

Who always

Supported and encouraged me.

TABLE OF CONTENTS

LIST OF FIGURES

LIST OF TABLES

ABSTRACT

This objective of this research is automatic detection and localization of myocardial infarction (MI) using back propagation neural networks (BPNN) classifier with features extracted from 12 lead ECG. Detection of MI aims to classify normal vs. infarcted subjects and localization is the task of specifying the infarcted region of the heart. The electrocardiogram (ECG) source used was the PTB database available on Physiobank. Time domain features of each beat in the ECG signal such as T wave amplitude, Q wave and ST level deviation, which are indicative of MI, were extracted. For localization, lead-wise principal components analysis (PCA) was done on the data extracted from ST-T region (0.4 seconds after the J point) and Q wave region (0.06 seconds around the start of QRS complex) of each beat. The resulting principal components were used as features for localization of seven types of myocardial infarction which were divided into two spatially related classes with class-1 comprising of Anterior, Antero-lateral and Antero-septal infarcts and class-2 comprising of Inferior, Infero-lateral, Infero-posterior and Infero-posterolateral infarctions. Localization into these two classes through classification would indicate the general region of the heart which has been infarcted. The feature dataset extracted from 148 records was divided into disjoint training, cross validation and testing data sets. For detection and localization separate neural network architectures were optimized using minimum cross validation error criterion over the cross validation data set after training. For detection, it was found that the sensitivity and specificity of BPNN for beat classification was 97.5 % and 99.1% respectively. For localization, PCA based features using back propagation neural network classifier resulted in a maximum beat classification accuracy of 93.7%. The proposed method due to its simplicity and high accuracy over the PTB database can be very helpful in correct diagnosis of MI in a practical scenario.

CHAPTER 1
INTRODUCTION

In the recent years, there is an increase of death rate due to cardiac diseases, early detection of such diseases is crucial because later diagnosis may not help in any treatment. Increased computing power has given the opportunity for implementing powerful diagnostic methods. Today, there are considerable commercial interests in the classification of electrocardiogram (ECG) signals. The overall research is aimed at developing a computerized system that categorizes ECG signals. ECG is one of the oldest and most popular instrument based measures in medical applications. Its most recent evolutionary step, to computer based systems, has provided a high resolution ECG that has opened new ways of ECG analysis and interpretation.

1.1 Research Objectives

The main purpose of the project is to develop a computer based offline ECG expert system for the automatic detection and localization of one of the most important heart diseases, that is, Myocardial Infarction (MI). The development of such a system would greatly aid medical experts in interpreting the ECG and making correct diagnostic decisions in case of MI by providing reliable feature extraction from ECG (such as Q wave detection and ST level deviation etc) saving time and effort of medical expert so that he/she can handle more number of MI patients simultaneously. The system will also enable physicians, who are not cardiac experts, to handle MI patients with ease and accurately. An experienced cardiologist can easily diagnose various heart diseases just by looking at the ECG waveforms but in some specific cases, sophisticated ECG analyzers can achieve a high degree of accuracy than that of the cardiologist. The use of computerized analysis of easily obtainable ECG waveforms can reduce the doctor's workload up to great extent.

Some analyzers assist the doctor by producing a diagnosis, other provides a limited number of parameters and by the help of those parameters the doctor can make his own diagnosis. The automatic decision support system comes out to be very useful in a country like Pakistan where the number of expert cardiologists is very less per unit of population.

1.2 System Modules

The different modules that comprises the overall system is shown in the figure 1.1 followed by a short description of each of them.
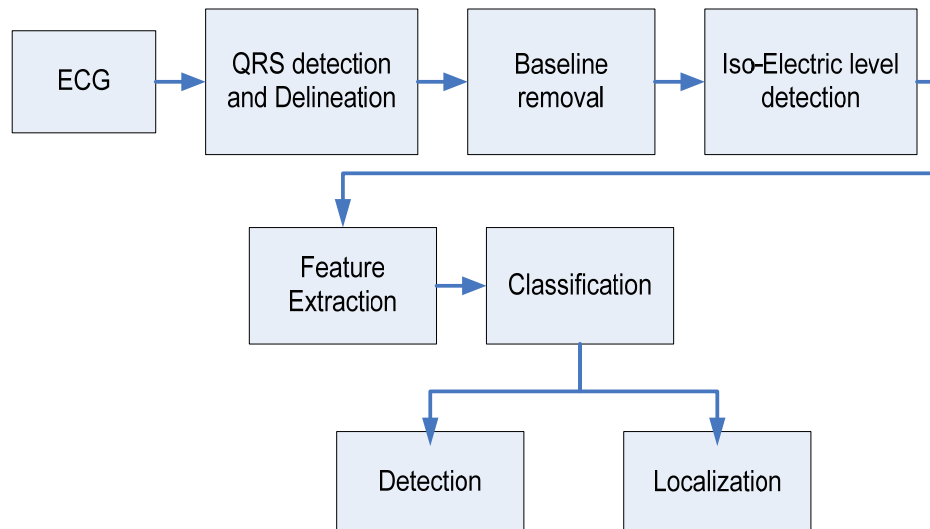
Figure 1.1 System Block Diagram

1.2.1 Signal Pre Processing

The raw ECG signal is taken from the PTB database and is pre processed. The pre processing tasks in this work are QRS delineation, Baseline removal and iso electric level detection as shown in the block diagram 1.1.

1.2.2 Feature Extraction

The pre processed signal is then used as input to feature extraction module where different features extraction techniques are implemented to extract MI describing features from ECG such as Q wave amplitude, ST level deviation and T wave amplitude. Such features indicate the presence or absence of MI.

1.2.3 Classification

In classification, there are two tasks that are implemented, that is, Detection of MI (It tells whether the subject is normal or abnormal) and Localization of MI (It gives information about the location of infarction).

1.2.4 Organization of the Thesis

This document presents the detail description of the work done in this project. The work description has been divided into different chapters/sections. Chapter 1 gives an introduction to the project. Chapter 2 describes ECG basics and gives an introduction to Myocardial Infarction, the heart disease on which we have focused in this project. Chapter 3 contains an overview of the characteristics of the PTB database used in this project plus ECG signal pre processing techniques. Chapter 4 explains the procedures for ECG feature in relation to time domain features such as ST level deviation etc and PCA based feature extraction where chapter 5 describes the implemented methods for classification such as back propagation neural networks (BPNN) in relation to Detection and Localization of MI. Chapter 6 has the details of classification results for detection and localization of MI by different datasets and different features extraction methods and chapter 7 presents conclusion and future work.

In this work, some of the existing implemented methods have been used as it is such as the ECG signal pre processing and QRS delineation, while some have been developed such as feature extraction algorithms and classification methods.

CHAPTER 2
ECG BASICS AND MYOCARDIAL INFARCTION

In this chapter we describe the heart structure and Electrocardiogram (ECG) formation. We give an overview of different components of ECG and describe what is myocardial infarction (MI), and introduces different types of MI with related changes in the ECG followed by a description of the detection and localization of MI.

2.1 The Heart and its function

The heart is the central structure of the cardiovascular system. The heart contains fours chambers and one way valves, as shown in the figure 2.1. A wall or septum divides the heart into left and right sides which are further partitioned into an upper chamber atrium and lower chamber ventricle. The right side of the heart receives the de-oxygenated blood which is pumped into lungs for getting oxygen and leaving carbon dioxide. The left side receives the oxygenated blood which is pumped to the whole body for oxygen distribution.
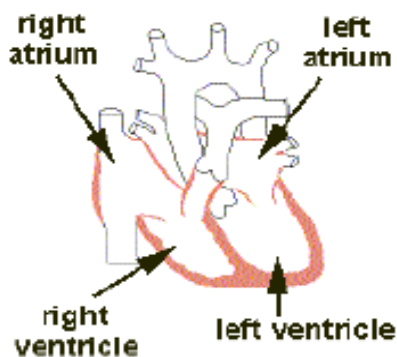
Figure 2.1 Major parts of the Heart

The contraction of the heart muscles enables the blood to be pumped. Myocardial cell can contract spontaneously under normal condition, these

contraction are triggered by the action potentials originating from the cells situated in two areas of the heart- the Sino-Atrial (SA) and Atrio-ventricular (AV) nodes. The SA node is the generally the site to trigger the action potential for heart-beat, but AV node can take this role if for some reason the SA node fails.

2.1.1 Conduction System of the Heart

This section gives an overview of the different parts of electrical pulse conduction system in the heart.

2.1.1.1 Sinoatrial Node (SA node)

The sinoatrial node (SA node) consists of a cluster of specialized cells that have pacemaker activity (automaticity). These cells are responsible for initiating the electrical impulse that stimulates the heart muscles to contract rhythmically. The SA node is located high on the right atrium close to where the superior vena cava enters the right atrium as shown in figure 2.2.
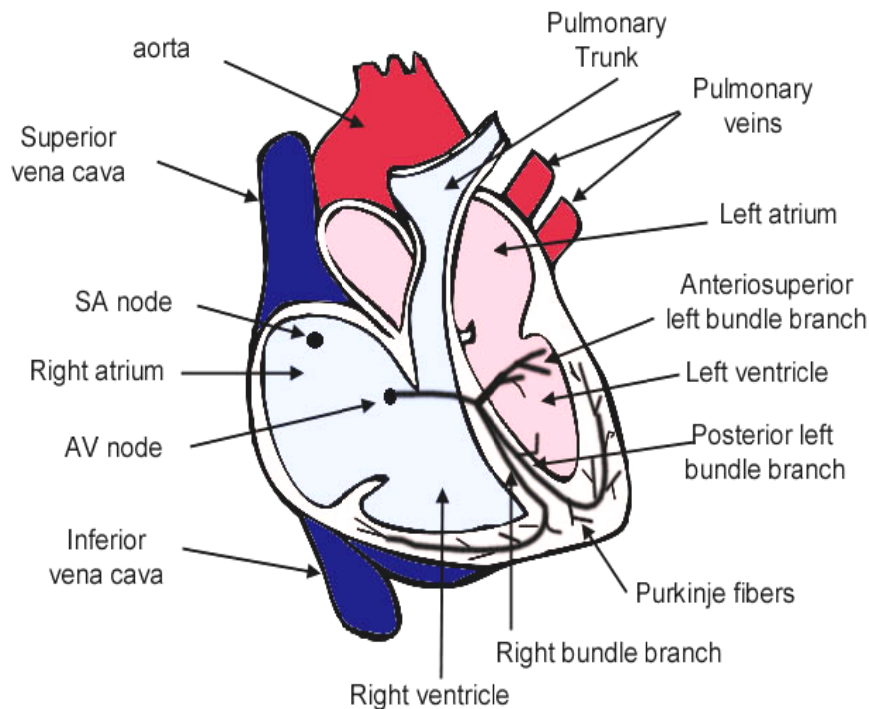
Figure 2.2 A view of the heart showing different parts

2.1.1.2 Sinus rhythm

The SA rhythm is the normal pacemaker of the heart, firing at about 60-100 beats per minute. A heart controlled by the SA node is said to be in normal sinus rhythm. The electrical impulse from the SA node spreads over the right and left atria and causes atrial contraction. The impulses are also conducted to the atrioventicular (AV) node. It takes about 0.03 seconds for the impulse to travel from the SA to AV node.

2.1.1.2 The Atrioventicular Node

Atrioventicular node (AV node) is located on the interatrial septum. It receives impulses from the SA node and conducts them to the bundle of His. Conduction through the AV node is slow providing a deliberate delay that allows the ventricles you fill up before the ventricles contract. The AV node provides the path of least resistance for the impulse to proceed to the ventricles.

2.1.1.3 Bundle of His

The bundle of His is located in the proximal intraventicular septum. It emerges from the AV node to begin the conduction of the impulse from the AV node to the ventricles. The Bundle of His branches into the right, left anteriosuperior and left posterioinferior bundle branches.

2.1.1.4 Bundle Branches & Purkinje Fibers

The bundle of His branches into the three bundle branches: the right, left anteriosuperior and left postrioinferior bundle branches that run along the interventicular septum. The bundles give rise to thin filaments known as Purkinje fibers. These fibers distribute the impulse to the ventricular muscle. Collectively, the bundle branches and purkinje network comprises the ventricular conduction system. It takes about 0.03-0.04s for the impulse to travel from the bundle of His to the ventricular muscle.

2.2 Electrocardiography

The various propagating action potentials within the heart produce a current flow, which generates an electric field that can be detected in significantly attenuated form at the body surface through a voltage measurement system. The resulting measuring measurement, when taken with electrodes in standardized locations, is known as the Electrocardiograph (ECG) which is in the range of +-2 MV. Each component of the ECG is directly related to the spread of electrical currents through specific regions of the heart (Fig. 2.3). Thus sufficient information is available in these signals to enable diagnosis of a number of cardiac abnormalities. The P wave is representative of atrial depolarization (cardiac stimulation), the QRS complex represents ventricular depolarization and the T wave represents the return of the ventricles to their resting state (re-polarization).
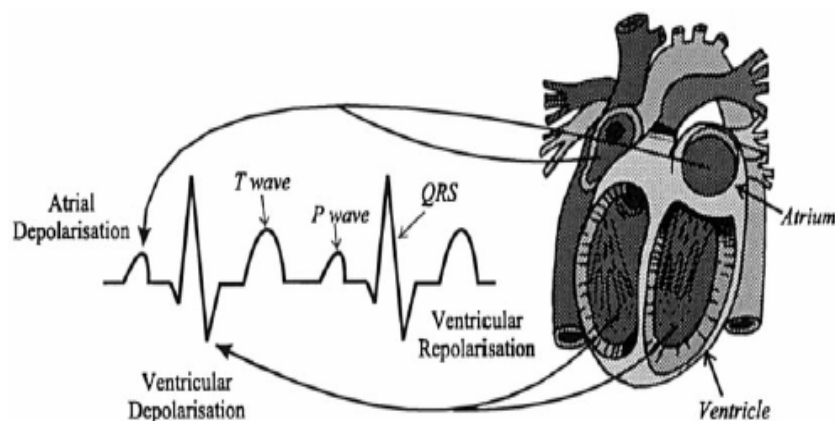
Figure 2.3 ECG formation

The standard 12-lead ECG system consists of four limb electrodes and six chest electrodes. These electrodes or leads view the electrical activity of the heart from 12 different positions, 6 standard limb leads and 6 pericardial chest leads as shown in the table 2.3. Each lead views the electrical activity from different angle and monitors specific portions of the heart from the point of view of positive electrode in that lead.

The ECG, over a single cardiac cycle, has a characteristic morphology as shown in Figure 2.4 comprising a P wave, a QRS complex and a T wave.

Table 1.1 ECG 12 lead system

Standard Leads	Limb Leads	Chest Leads
Bipolar Leads	Unipolar Leads	Unipolar Leads
Lead I	AVR	V1,V2,V3
Lead II	AVL	V4,V5,V6
Lead III	AVF	

The normal ECG configurations are composed of waves, complexes, segments, and intervals recorded as voltage (on a vertical axis) against time (on a horizontal axis). A single waveform begins and ends at the baseline. When the waveform continues past the baseline, it changes into another waveform. Two or more waveforms together are called a complex. A flat, straight, or isoelectric line is called a segment. A waveform, or complex, connected to a segment is called an interval. All ECG tracings above the baseline are described as positive deflections. Waveforms below the baseline are negative deflections. Subsequent sections describe ECG waves and intervals in detail.
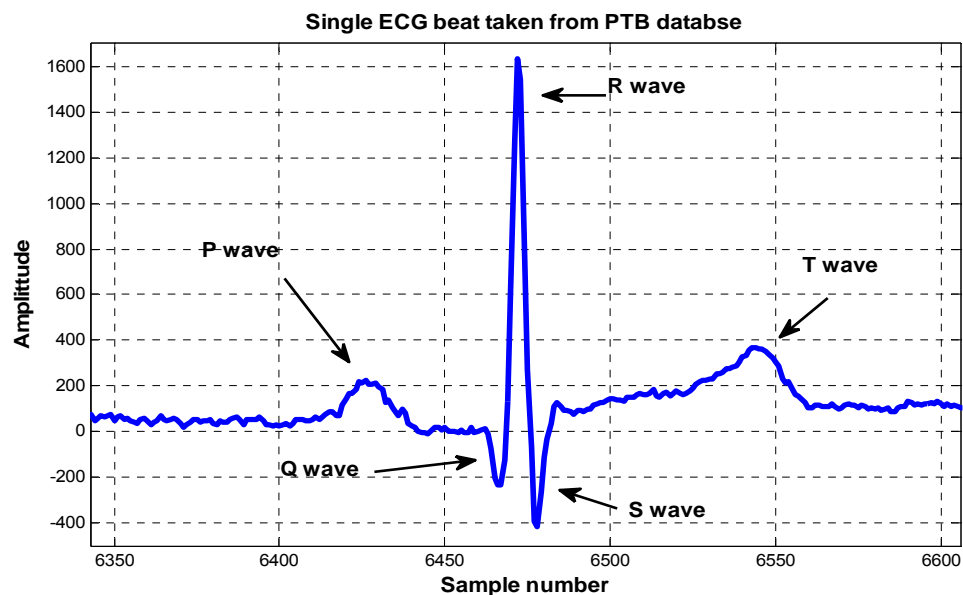
Figure 2.4 ECG beat from PTB database showing different components such as P wave, QRS complex and T wave

2.2.1 P Wave

The onset of depolarization in the heart is seen in SA node, an area at the upper right border of the heart consisting of pace maker cells. A wave of depolarization travels from SA node, downward, leftward and posteriorly, trough both atria, depolarizing each cell in its turn. This can be seen as the P wave in the ECG (See figure 2.5 for p wave formation). The magnitude of the P (shown in figure 2.4.) wave is normally low (50-100uV) with about 100 millisecond duration.
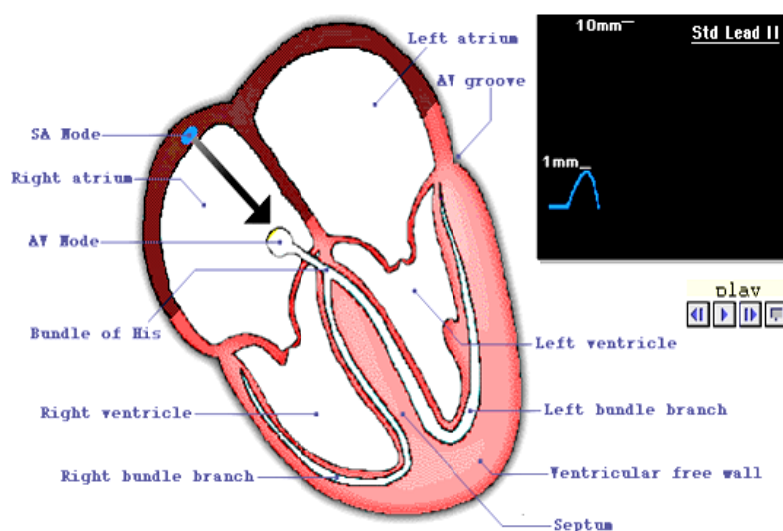
Figure 2.5 P wave formation in ECG waveform

2.2.2 The QRS complex

The QRS complex corresponds to the period of ventricular contraction or depolarization. It is the result of ventricular depolarization through the Bundle Branches and Parkinje fiber. In this portion of the beat we can see three different waves i.e. Q wave, R wave and S wave as shown in figure 2.6. QRS can be measured from the beginning of the first wave in the QRS (start of Q wave) to where the last wave in the QRS returns to the baseline (end of S wave). Normal measurement for QRS is 60ms-100ms.
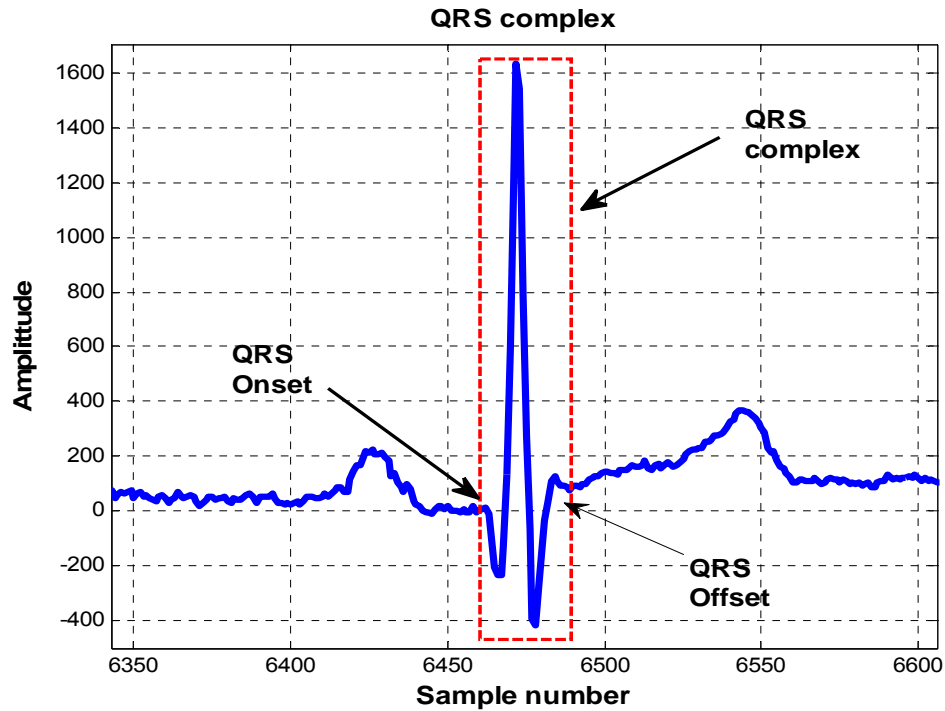
Figure 2.6 Q, R and S waves forming QRS complex

2.2.3 The ST segment

The ST segment represents the time between the ventricular depolarization and the re-polarization. The ST segment begins at the end of the QRS complex and ends at the beginning of the T wave. Normally, the ST segment measures 0.12 second or less.

2.2.4 The T wave

The T wave results from the re-polarization of the ventricles and is of a longer duration than the QRS complex because the ventricular re-polarization happens more slowly than depolarization. Normally, the T wave has a positive deflection of about 0.5mv, although it may have a negative deflection. The duration of the T wave normally measures 0.20 second or less. It is shown in the figure 2.7.
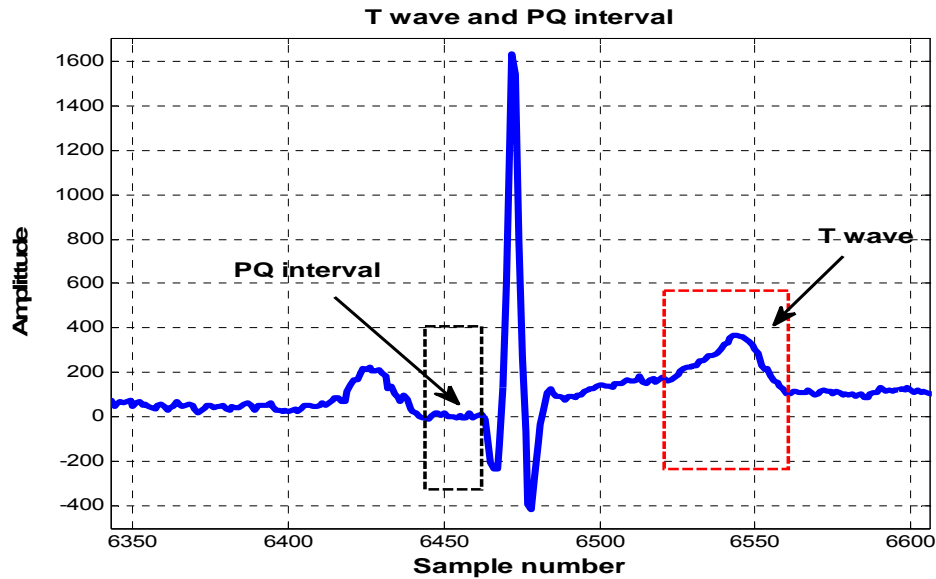
Figure 2.7 T wave and PQ interval

2.2.5 The QT interval

The QT interval begins at the onset of the Q wave (QRS start point) and ends at the endpoint of the T wave, representing the duration of the ventricular depolarization/repolarisation cycle.

2.3 Myocardial Infarction (MI)

Heart attack (also known as a myocardial infarction) is caused by death of the heart muscle due to sudden blockage of a coronary artery by a blood clot. Coronary arteries are blood vessels that supply the heart muscle with blood and oxygen. Blockage of a coronary artery deprives the heart muscle of blood and oxygen, causing injury to the heart muscle. Injury to the heart muscle causes chest pain and chest pressure sensation. If blood flow is not restored to the heart muscle within 20 to 40 minutes, irreversible death of the heart muscle will begin to occur. Muscle continues to die for six to eight hours at which time the heart attack usually is "complete." The left ventricle is the thickest chamber of the heart; so if the coronary arteries are

narrowed, the left ventricle (which uses the greatest blood supply) is the first to suffer from an obstructed coronary artery. When we describe infarcts by location, we are speaking of an area of the left ventricle. Coronary arteries to the left ventricle usually send smaller branches to other regions of the heart, so an infarction of the left ventricle can include a small portion of another chamber. Besides cardiac arrhythmias, myocardial infarction (MI) represents the most important subject in electrocardiography due to its severity and prevalence. MI can be recognized by typical ST level deviation, significant Q wave and T wave inversion. Approximately 70% of MIs are recognizable in the ECG, based on well-defined criteria. Approximately 30% of acute and previous MIs are not recognizable in the ECG. The reasons are: 1. Small infarctions; 2. Infarctions associated with left bundle-branch block (LBBB); 3. Multiple infarctions, and one infarction pattern masks the other and last 4. Electrocardiography is an indirect method. It is therefore astonishing that so many MIs are recognized in the ECG, in many cases with reliable determination of localization.

2.3.1 ST, Q, and T Vectors in Myocardial Infarction

The infarction pattern at any stage appears in the directly detecting leads, this fact greatly simplifies the diagnosis of MI. The injury (lesion) ST vector points to the region of infarction, resulting in ST elevation as shown in figure 2.8 (a).
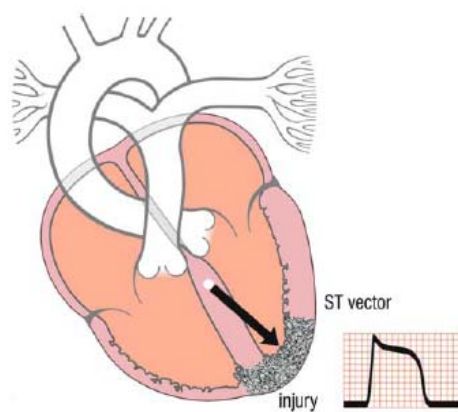
(a)
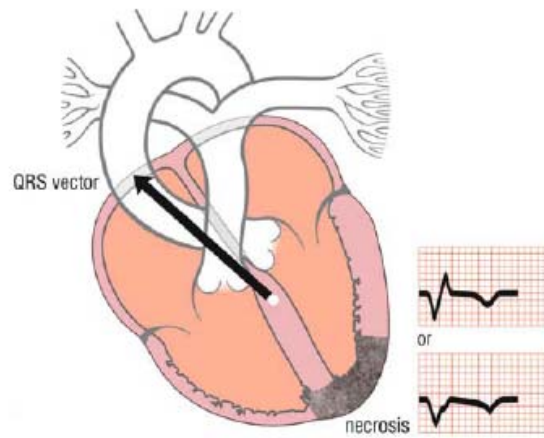
(b)
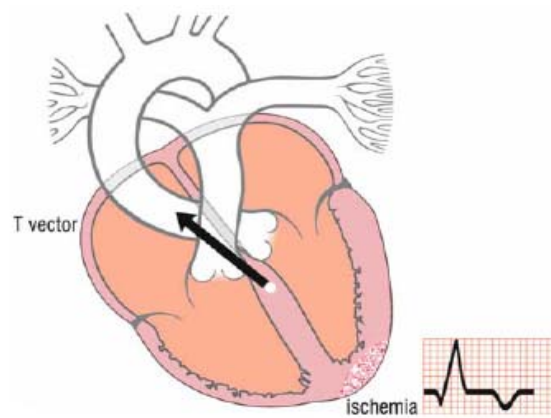
(c)

Figure 2.8 ST, QRS, and T vectors in myocardial infarction. a. ST injury vector. b. QRS vector in necrosis. c. T ischemia vector

The necrosis QRS vector points to the opposite direction of the infarcted area, producing a pathologic Q wave or QS wave (Figure 2.8b). The ischemia vector also points away from the infarction zone, resulting in negative and symmetric T waves (Figure 2.8c). The two stages of MI evolution according to the international nomenclature are:

- Acute stage: ST elevation with or without pathologic Q waves

- Subacute and old stage: Pathologic Q waves, isoelectric ST segment

The ST elevation with or without pathologic Q waves corresponds to AMI, and pathologic Q waves with isoelectric ST segment (with or without negative T waves) to subacute MI and at the same time to an old MI.

As for as MI localization is concerned, the infarction pattern indicate itself in different leads of ECG. The localization can be easily determined from the three dimensional exploration of the cardiac vectors produced by 12 standard ECG leads. The relationship between the localization of infarction and the exploring leads is described in subsequent sections together with the most frequent localizations of coronary artery obstruction, for each infarction localization.

2.3.2 Anteroseptal Infarction

As leads V2 and V3 are placed over the interventricular septum, and V4 over the apex, anteroseptal infarction (Figure 2.9) will produce the typical pattern in these leads (also in V1), according to the infarction stage Leads V2, V3 and also V1 shows these changes (figure 2.10).
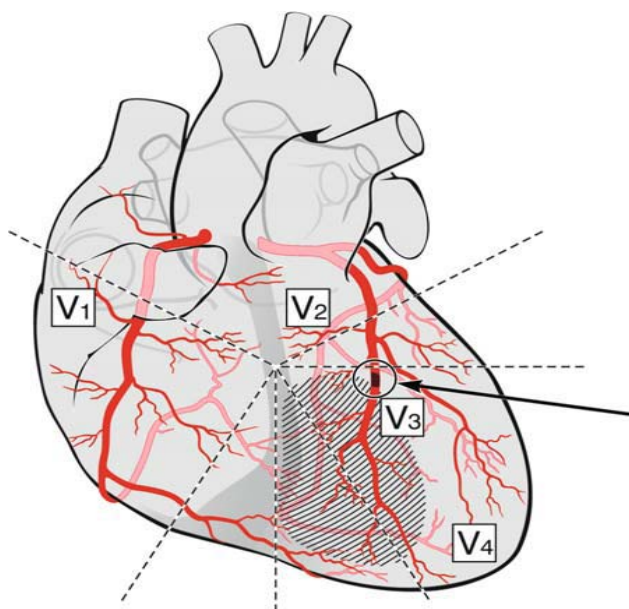
Figure 2.9 Site of anteroseptal MI

ST elevation in Antero Septal MI

(a) ST elevated in V1

Lead V2 [from PTB databse]
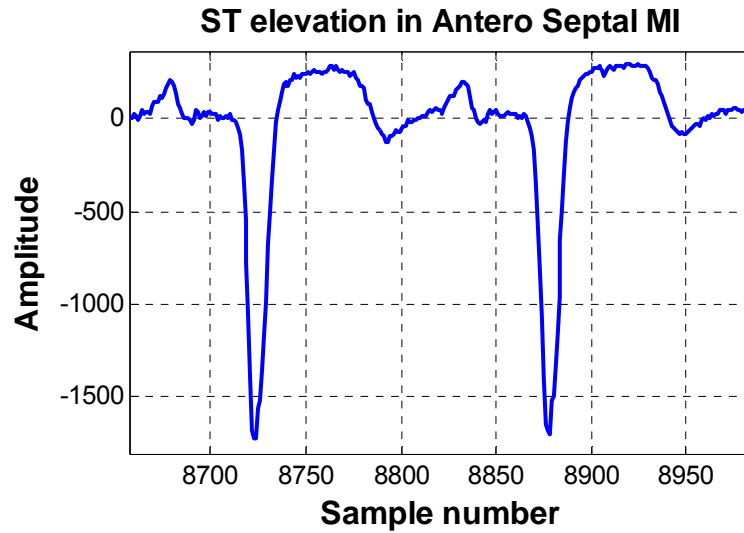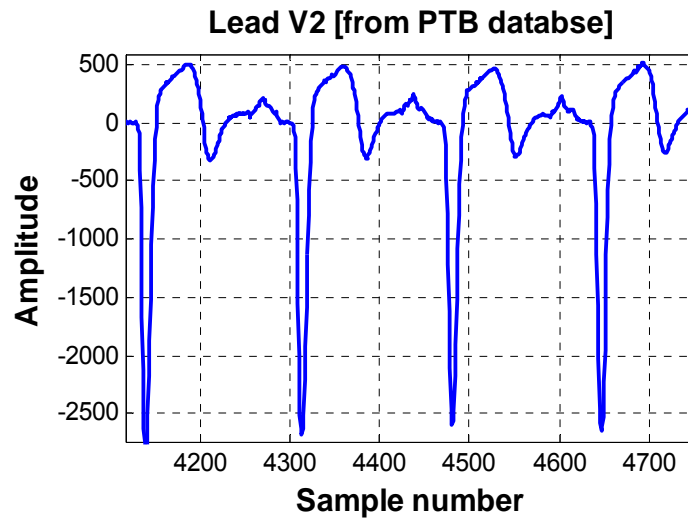
(b) Lead V2 from a patient having AS MI

Figure 2.10 ST elevations in anteroseptal infarction

2.3.3 Lateral Infarction

This infarction is rare in its isolated form (figure 2.11). Leads V5 and V6 directly explore the lateral wall; the typical pattern in these leads is seen. Depending on the infarction size, the typical signs might also be present in leads I and aVL. In high lateral infarction, the best directly exploring lead is aVL.
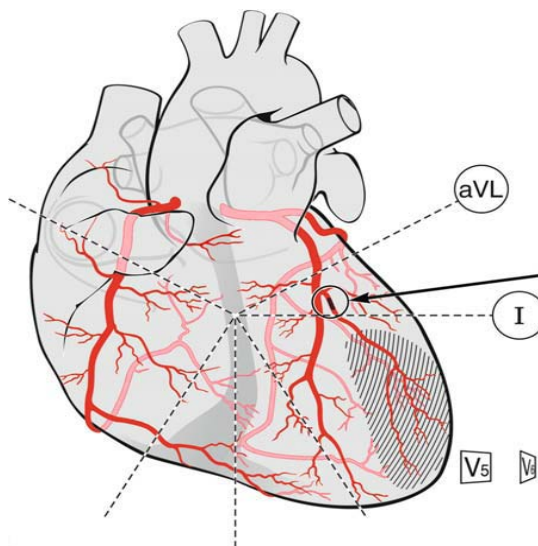
Figure 2.11 Site of lateral infarction

2.3.4 Anterolateral Infarction

Anterolateral infarction includes infarction of the septum, the apex, and lateral portions of the left ventricle (figure 2.12). The infarction pattern can be seen in the leads (V1) V2 to V4, in lead V5, and often V6.
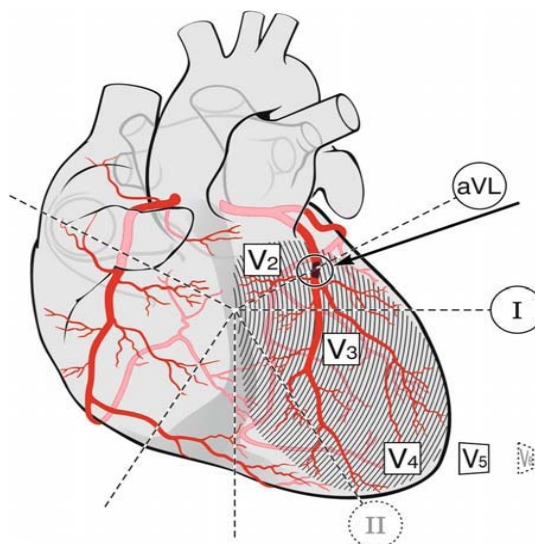
Figure 2.12 Site of AneroLateral MI

In this infarction type, the pattern is also detected by leads I and aVL (in aVL if the high lateral portion of the left ventricle is involved). ECGs 2.13 a-c are examples of anterolateral MI.
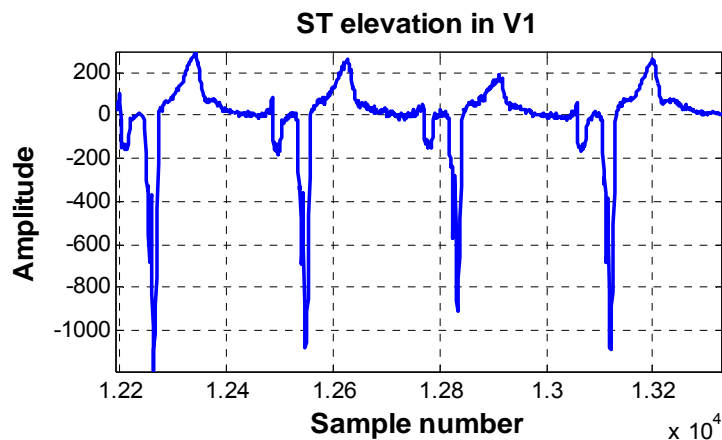
ST elevation in V1

(a) ST elevation in Lead V1 (PTB database)

ST elevation and T wave inversion
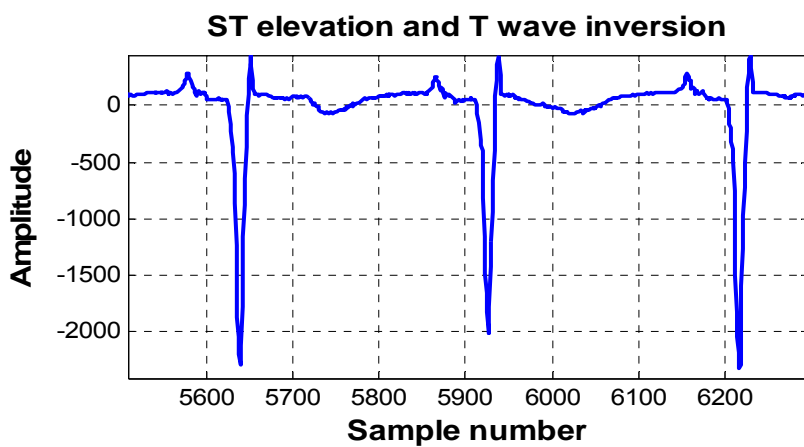
(b) ST elevation and T wave inversion in Lead V3 (PTB database)

T wave inversion in V4
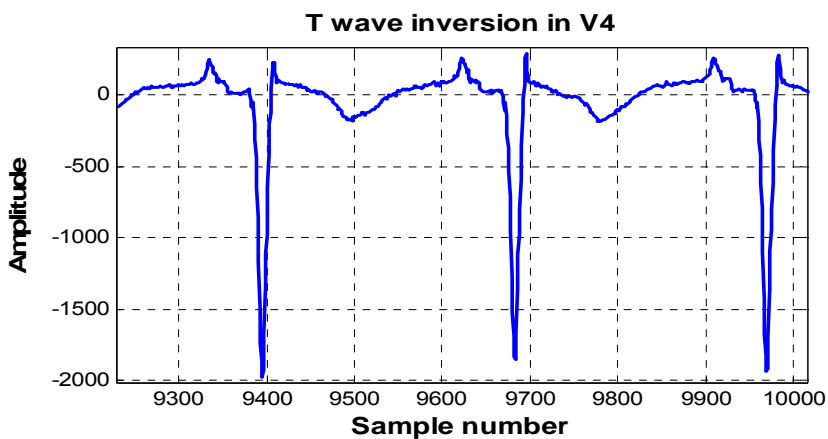
(c) T wave inversion in Lead V4 (PTB database)

Figure 2.13 Leads V1, V3 and V4 From anterolateral MI subject (PTB database)

2.3.5 Inferior Infarction

The pattern of inferior infarction is detected in leads II, III and aVF (figure 2.14). In practice, the alterations are best seen in leads aVF and III, less distinctly in lead II. However, a q wave also in lead II favors the diagnosis of inferior infarction. ECGs taken from PTB database shows some of these changes (figure 2.15).
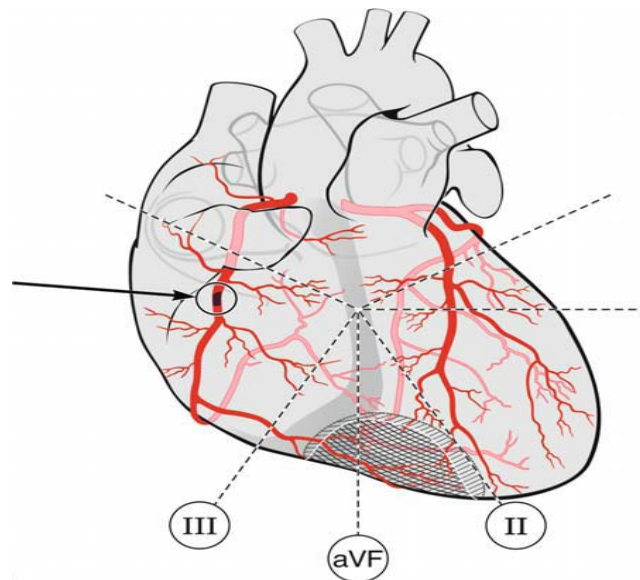
Figure 2.14 Site of Inferior infarction
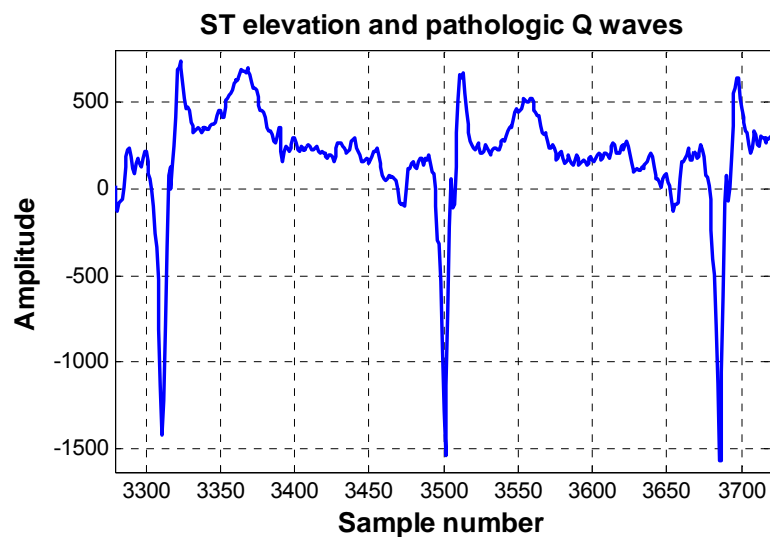
(a) Lead III (Inferior MI from PTB patient #078)
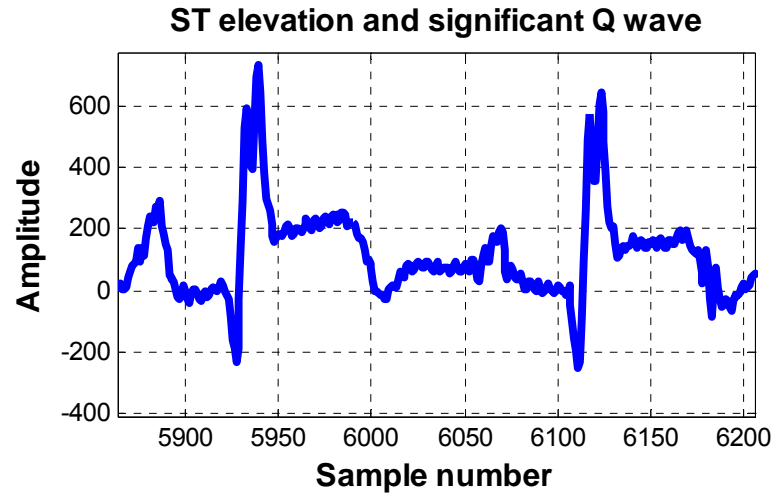
ST elevation and significant Q wave

(b) Lead II (Inferior MI from PTB patient #026)

ST elevation, negative T wave

(c) Lead III (Inferior MI from PTB patient #026)

ST elevation and negative T wave in aVF
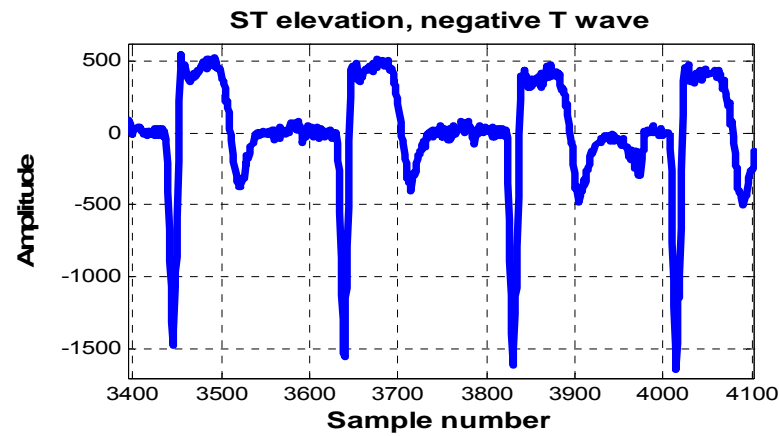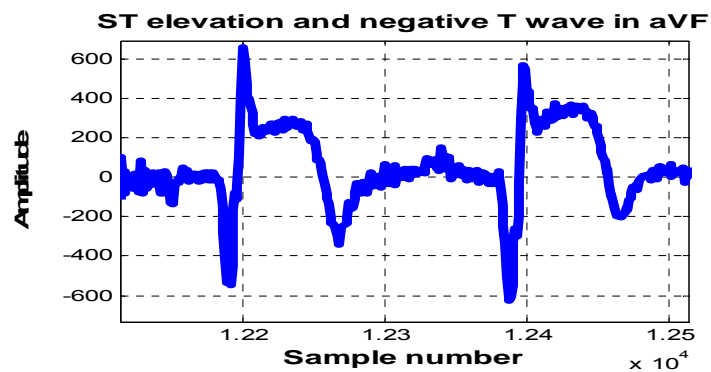
(d) Lead III (Inferior MI from PTB patient #026)

Figure 2.14 a-d Electrocardiogram (ECG) obtained from PTB database with inferior myocardial infarction. Pathologic Q waves, ST elevation, and T wave inversion in leads II, aVF, and III.

2.3.6 Posterior Infarction

For one particular reason, this infarction pattern is difficult to understand. According to the definition of pathologic Q waves, and referring only to the 12 standard ECG leads, the pattern is not a Q wave infarction (figure 2.16). We only see the mirror image of the original pattern in some of these leads. The additional posterior leads V7, V8, and V9 provide the direct infarction pattern. The mirror image is seen in the opposite leads, the anterior (anteroseptal) leads V2 and V3, and sometimes V1, consisting of an ST depression instead of an ST elevation and/or a great and broad R wave instead of a broad Q wave, depending on infarction stage.
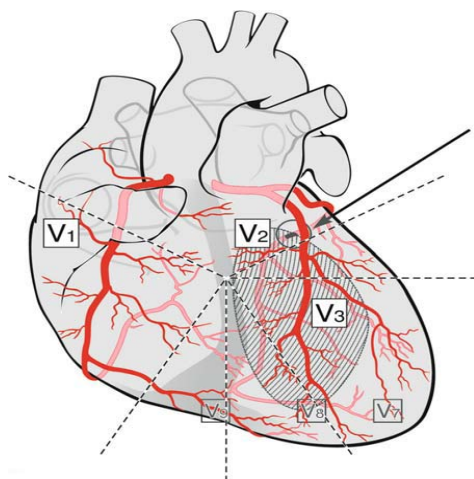
Figure 2.16 Posterior Infarction

In absence of pathologic Q waves and/or ST elevation in the 12 standard leads, the possibility of infarction is often not considered. Thus, in the presence of the following alterations in leads V1 to V3, the diagnosis of posterior infarction should always be confirmed or excluded with the help of leads V7 to V9:

1. Single R wave and/or an Rs complex, with an R duration of ≥ 0.04 s

2. Isolated ST depression

3. Combination of 1 and 2

ECGs in figure 2.17 show some changes. Abnormal R wave and ST deviation in leads V1 and V3.
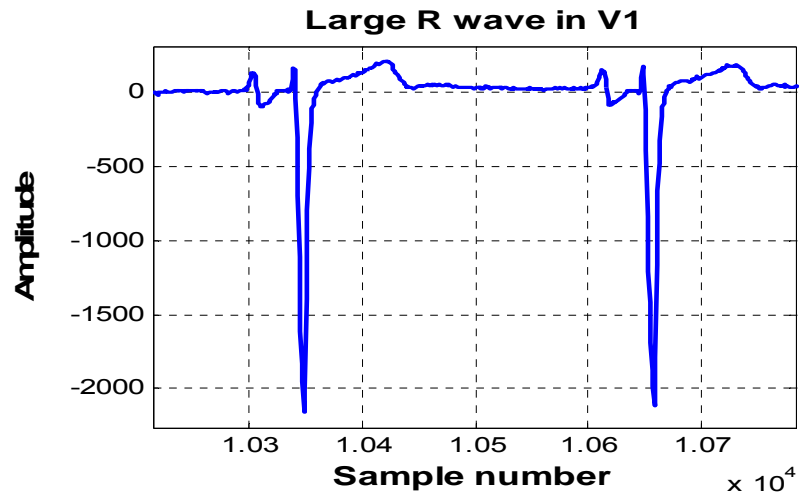
(a) Lead V1 ECG from PTB patient#85 with posterior MI
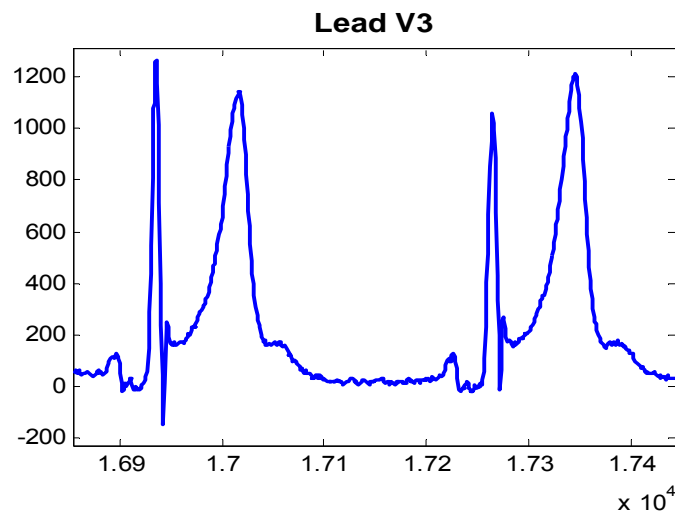
(b) Lead V3 ECG from PTB patient#85 with posterior MI

Figure 2.17 a-b Leads V1 and V2 ECGs from PTB

2.3.7 Anterior Infarction

In this case the site of infarction is the anterior wall of the left ventricle (Anterior left coronary artery). Q waves in chest leads V1, V2, V3, or V4 signify an anterior infarction. ECGs taken from PTB database in figure 2.18, shows an anterior infarction in the specified leads with ST elevation , T wave inversion and abnormal Q wave.
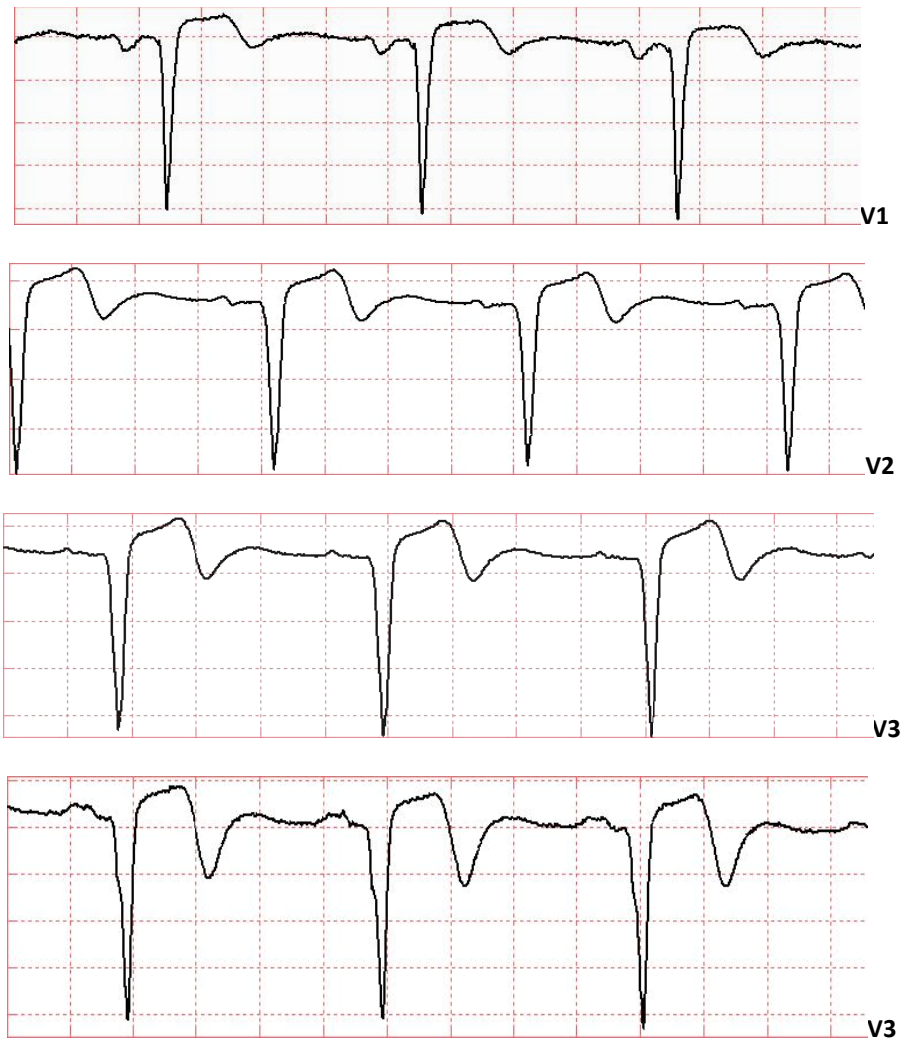
Figure 2.18 ECGs Showing ST level elevated, T wave negative in anterior infarct

CHAPTER 3
ECG SIGNAL PRE PROCESSING

In this project the ECG source used, is the PTB database available on Physiobank [1]. The PTB database contains significant number of subjects with myocardial infarction on which we applied the techniques to get the simulated results. This section gives an overview of PTB database and describes in detail, the pre processing techniques for ECG that we applied.

3.1 The PTB database

PTB diagnostic ECG database is available free on the Physiobank, a good resource for obtaining biomedical signals. PTB Diagnostic ECG database provides datasets of infracted patients as well as healthy subjects. The PTB database contains 549 records collected from 294 subjects. Each subject is represented by at minimum one and maximum up to five records. Out of 294 subjects, the number of subjects that have been categorized as MI patients is 148. In the database the header files contain the clinical summary of the patient and .dat files contain the patient's actual ECG data. The Summary of the diagnostic classes of the subjects is given below.

Table 3.1 Diagnostic classes of the subjects in PTB database

S.No	Diagnostic class	Number of subjects
1.	Myocardial infarction	148
2.	Heart failure	18
3.	Bundle branch block	15
4.	Dysrhythmia	14
5.	Hypertrophy	7
6.	Valvular heart disease	6
7.	Myocarditis	4
8.	Miscellaneous	5
9.	Healthy controls	54

Within each record there are 15 leads/channels and each ECG signal contains different number of beats recording across the patients. A summary of the total number of beats in each type is given below.

Table 3.2 Number of beats of infracted and healthy subjects calculated from PTB

S No.	Type	Sub Type	Number of beats
1.	Healthy control	Normal	9491
2	Infarction	Anterior	7466
3	Infarction	Antero Septal	11700
4	Infarction	Antero lateral	6913
5	Infarction	Inferior	11591
6	Infarction	Posterior	467
7	Infarction	Lateral	466
8	Infarction	Postero Lateral	982
9	Infarction	Infero posterior	356
10	Infarction	Infero Lateral	8345
11	Infarction	Infero Postero Lateral	2634

The Table 2.2 shows that sufficient numbers of training and testing beats/examples are available for each type. In case of posterior and lateral, the numbers of beats are less as compared to others because there is one subject each in these types and this presents a difficulty in training the classifier for separating these types especially in case of localization. Each record includes 15 simultaneously measured signals: the conventional 12 leads (i, ii, iii, avr, avl, avf, v1, v2, v3, v4, v5, v6) together with the 3 Frank lead ECGs (vx, vy, vz). As for as myocardial infarction is concerned we just need the 12 leads data/ECG because the myocardial infarction is reflected in these 12 leads ECG [10].

3.2 ECG Signal Pre Processing and QRS Delineation

The raw ECG from the PTB database is then pre processed. The pre processing stages are shown in the figure 3.1 i.e. QRS detection and delineation, Baseline removal, and Iso electric level detection. Each of these techniques is described in detail in subsequent sections.
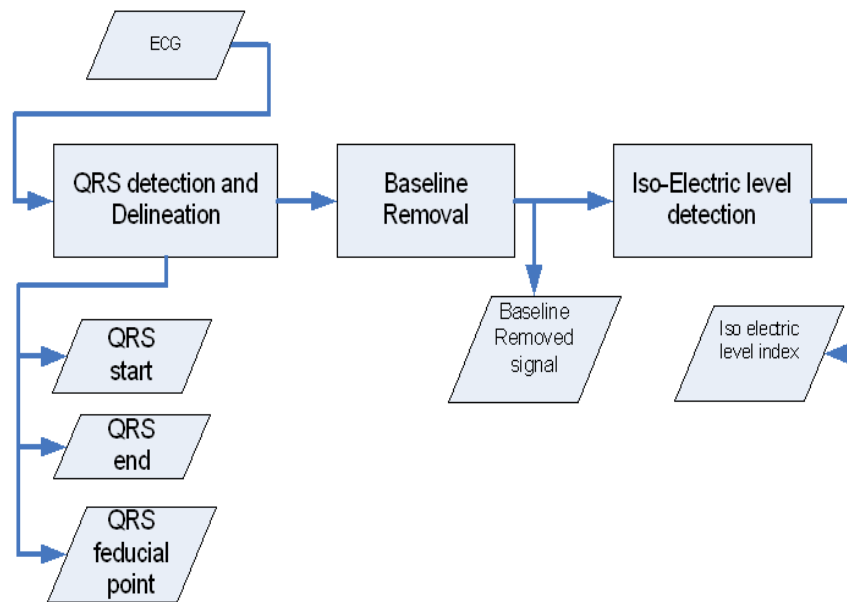
Figure 3.1 ECG segmentation and pre processing steps block diagram

3.2.1 QRS Detection and Delineation

At pre processing stage QRS detection and delineation is performed first, which has some major objectives such as determining the QRS start point, the QRS end point and the QRS feducial point. We need these points to use them as reference when doing baseline removal and further signal segmentation in feature extraction process.

QRS detection and delineation was done using an already implemented technique based on discrete wavelet transform (DWT) [11]. The algorithm keeps track of the signal derivative information (zero crossing and threshold) to determine a wave's start, peak point and end point as shown in the figure 3.2. Due to high accuracy of this method, it was used in this work.
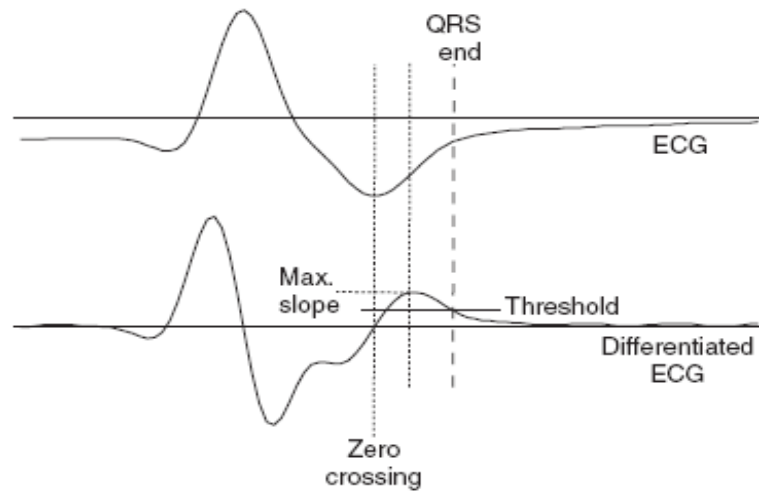
Figure 3.2 QRS delineation procedure based on differentiation and thresholding

The figure 2.3 shows the QRS delineation points generated by the adopted method for each beat when applied on ECG signal from PTB database.
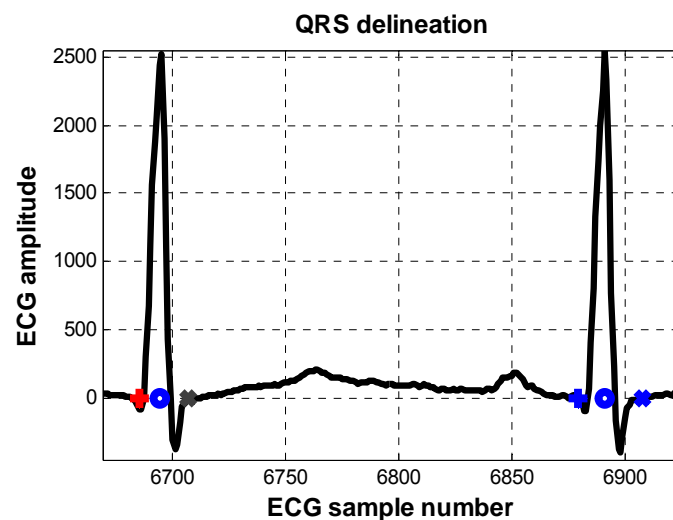
Figure 3.3 QRS delineation locating onset, offset and feducial point

3.2.2 Baseline Removal

Baseline wander is an extraneous, low-frequency artifact in the ECG (Figure 3.4a) which may interfere with the signal analysis, and makes the clinical interpretation inaccurate and misleading. When the baseline wander is there in the signal, the iso-electric line is not well defined and hence accurate measurements of the parameters which are considered relative to the iso-electric level can't be made. Baseline wander results from noise sources such as perspiration, respiration, body movements, and poor electrode contact. The magnitude of the undesired wander may exceed the amplitude of the QRS complex by several times [2]. Its spectral content is usually confined to a frequency band below 1 Hz, but it may contain higher frequencies as well.
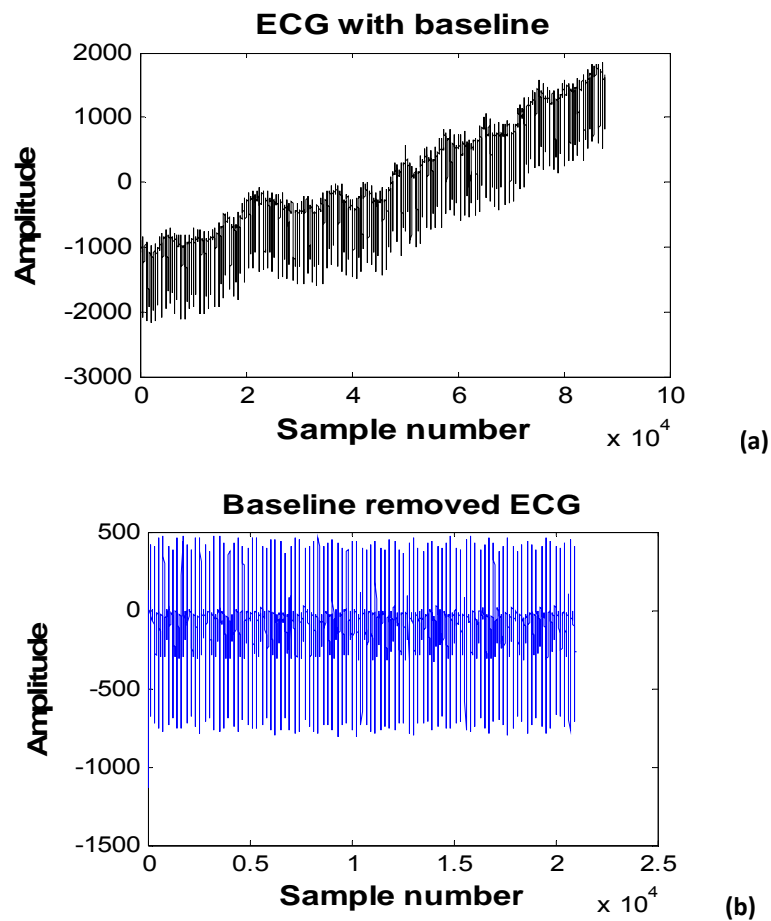
Figure 3.4 Cubic Spline Fitting for Baseline Removal. ECG with baseline (a) Baseline removed ECG (b)

A number of different techniques have been implemented for baseline wander removal [3] and [5]. We have used the cubic Spline based technique for baseline removal [3]. This method takes the ECG signal along with QRS delineation points such as QRS onset as inputs. This baseline removal method finds the knots (i.e. the flattest point in the PQ region) as the reference point and fits a third order cubic spline polynomial on those knots to obtain the baseline estimate which is then subtracted from ECG signal to get baseline removed signal. Figure 3.4 shows the ECG from PTB database with baseline (a) and with baseline removal (b). The baseline shown in figure 3.4 b presents a linear behavior but the method works also for the signals which show complex trend in baseline.

(a)

(b)
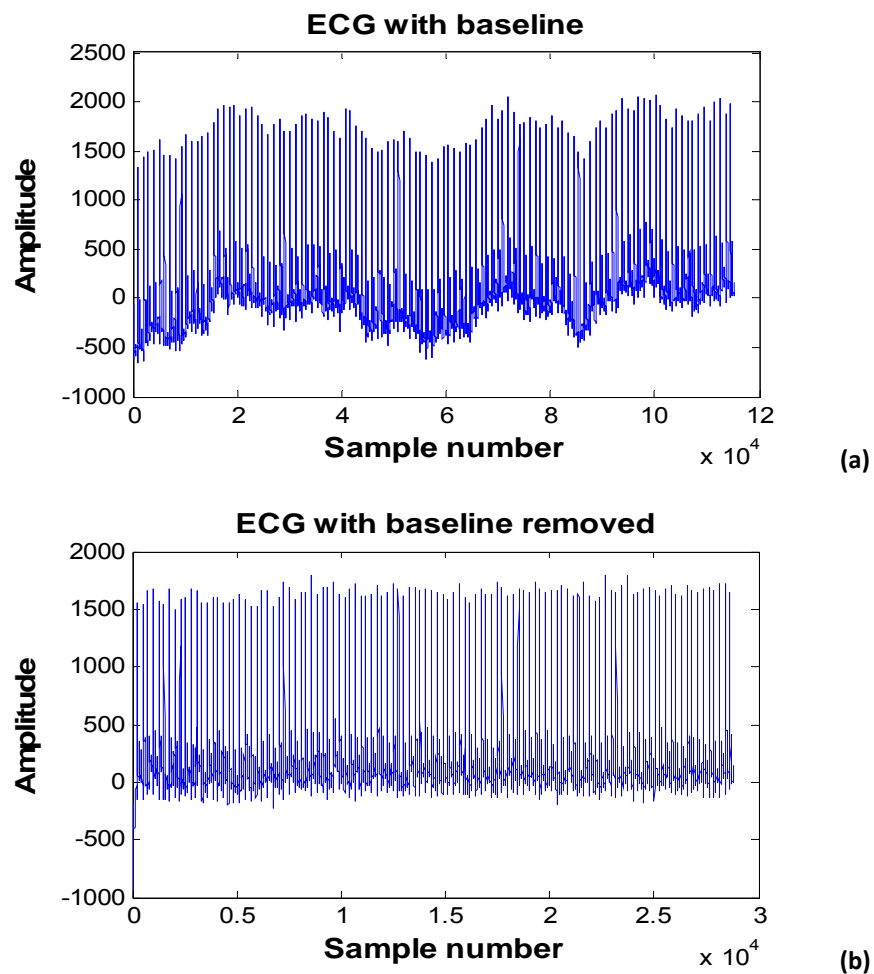
Figure 3.5 Complex baseline pattern (a) Baseline removal (b)

3.2.3 Iso electric level detection

The region after the end of the P wave and before the start of the QRS complex is known as the PQ region and it can be used to locate the iso electric level. The mean value of the flattest region in the PQ interval was considered as the iso electric level. The iso electric level detection is required because the ECG amplitude at different positions in the beat is measured relative to the iso electric level.

The procedure that was applied, searches the flattest region (where the absolute value of the slope is minimum) about 60 millisecond backward from the start of the QRS complex [6]. The procedure divides the search space into small windows and the line in each window is approximated with a first order polynomial then the slope of the line is calculated and the window with minimum slope (the window with slope close to zero) is selected to be the flattest region. The mean value of the selected window is taken as the iso electric level. In the figure 3.5 small dots show the iso electric level points that were detected by the algorithm. Time domain features as described in the next section are extracted using iso electric level points as a reference point in each beat i.e. measurements such T wave amplitude, Q wave amplitude and ST level elevation and depression are taken relative to iso electric level. The value of the signal at the iso electric level is calculated and then subtracted from the corresponding detection point (T or Q or ST) value in that beat.
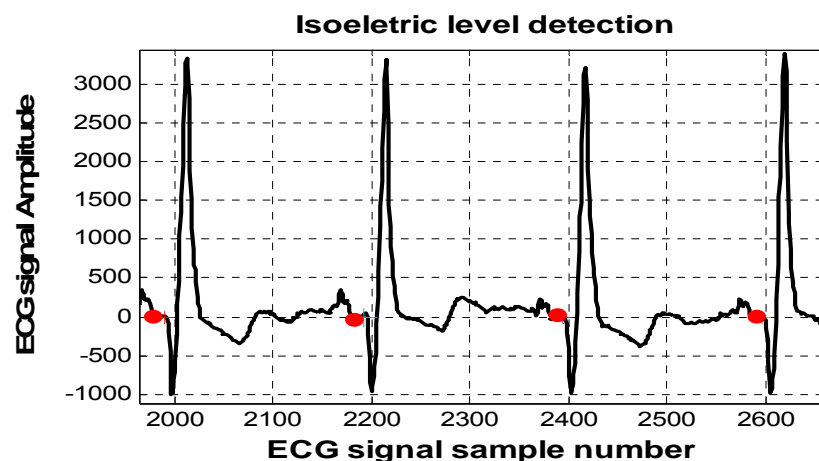
Figure 3.6 ECG Iso electric level detection (Source: PTB database)

CHAPTER 4
ECG FEATURE EXTRACTION

According to MI experts [11], the presence or absence of myocardial infarction is characterized by specific waves or segments in the ECG beats as discussed in detail in chapter 2. The main indicators are Q wave, T wave and ST level elevation or depression [11]. So we can either use the ECG amplitudes at these points or take the regions of the beat where these waves are most probably located. This led us to two approaches i) Time domain features and ii) Principal component analysis (PCA) as shown in the block diagram 4.1.
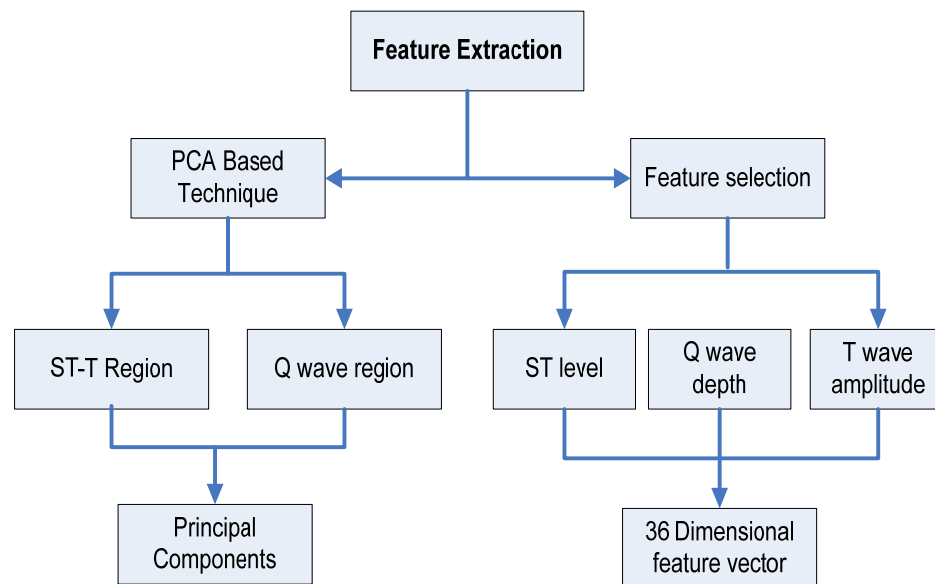
Figure 4.1 Feature extraction approaches, time domain features and PCA based features

4.1 Time Domain Features

Electrocardiographically two types of myocardial infarction exist [11] i.e. Q wave infarction which is diagnosed by the presence of Q waves and Non Q wave infarction, which is diagnosed in the presence of ST depression and T wave

abnormalities. The ECG has been used to localize the site of ischemia and infarction. Some leads depict certain areas; the location of the infarct can be detected accurately from analysis of the 12-lead ECG [11]. Therefore the time domain feature that has been used are Q wave amplitude, ST level deviation and T wave amplitude.

4.1.1 ST Deviation Measurement

ST segment is from the end of the QRS complex to the start of the T wave. ST elevation is usually measured 60 or 80ms after the J point depending on heart rate. We extract the ST segment using QRS end point and T wave start point or we can take directly the elevation point 80ms [7] after the J point which in accordance with the resample frequency 250 comes out to be 15 -17 samples after the J point. Figures 4.2 shows ST level detection points in each beat.
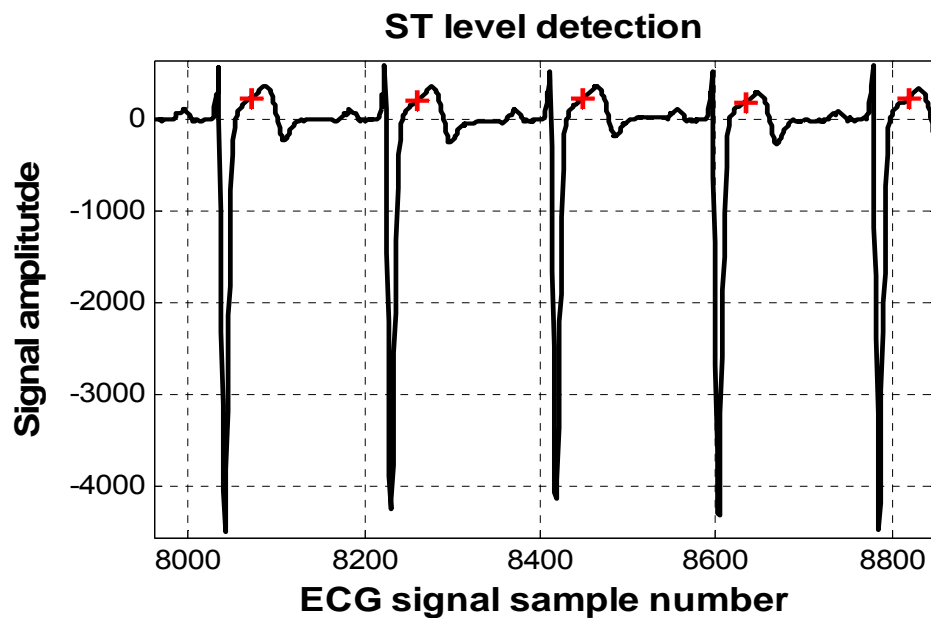
ST level detection

Figure 4.2 ST level detection points

After locating the ST level point, ST deviation is measure with respect to the iso electric level. The value of ECG signal at iso electric level is subtracted from the ECG value at the ST locating point to get the ST level measure for each beat; this becomes our first time domain feature.

4.1.2 Q Wave Detection and Amplitude Measure

The DWT based QRS detector described in chapter2 is was used for the detection of Q wave also. The procedure returns the indices where Q wave is present in the beat, and return 0 if Q wave is absent from the beat. By using the Q wave detection indices, Q wave amplitude is measure easily by taking the value of ECG at the Q wave detection point minus the ECG value at iso electric level for each beat. Figure 4.3 shows Q wave detection points as dots generated by the QWT based detector applied on ECG signal from PTB database.
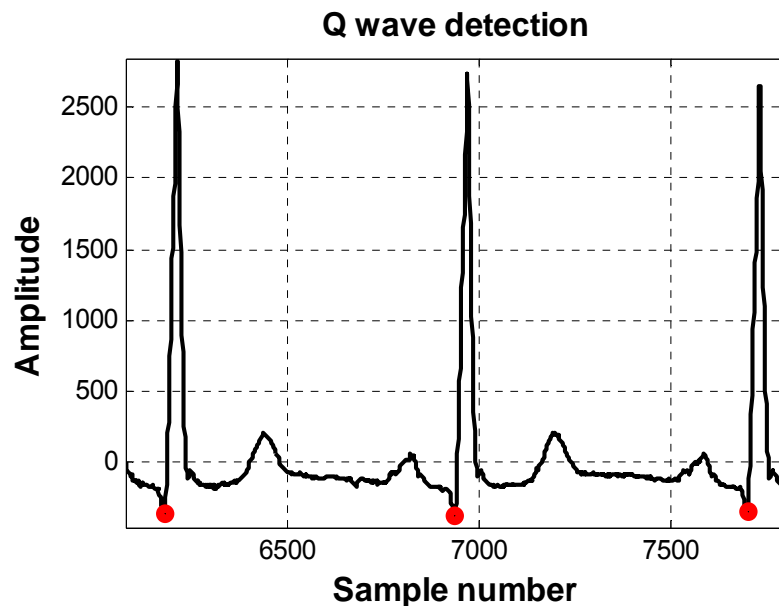
Figure 4.3 Q wave detection points shown as dots

4.1.3 T Wave Detection and Amplitude Measure

To determine T wave amplitude, a T wave delineator which has been implemented using discrete wavelet transform [3] has been used. The procedure finds the T wave onset and offset and gives the T wave start and end indices in ECG for each beat. Using onset and offset information, the T wave amplitude is calculated. T wave amplitude can be calculated by finding extreme value (minimum

in case of negative or inverted T wave and maximum in case of positive T wave) in the T wave start and T wave end region or alternately the point where the derivative of the curve (slope) is zero can be considered as T wave peak. The ECG in figure 4.4 shows the locating of T wave peak points and T wave amplitudes.
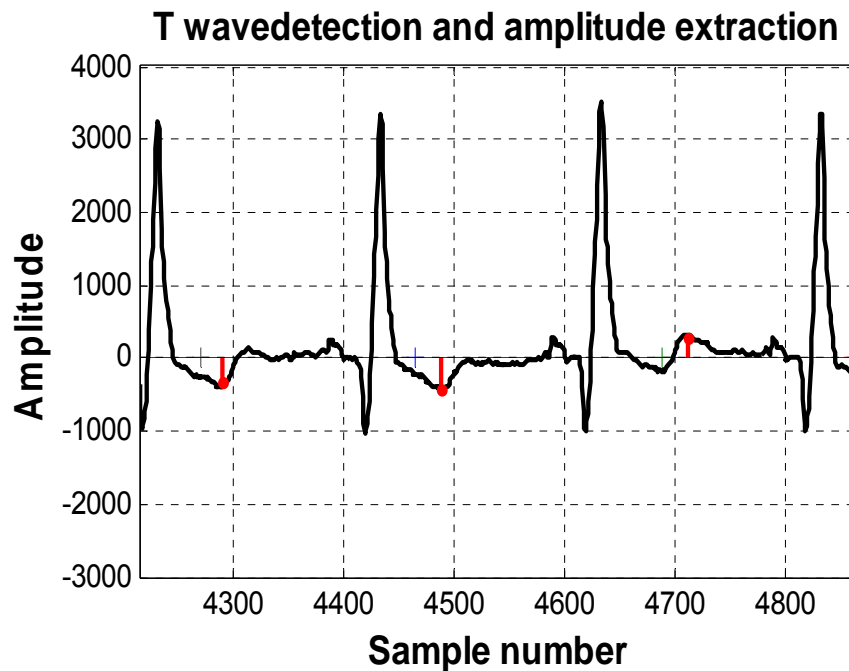
Figure 4.4 T wave detection and amplitude extraction

The above mentioned three time domain features i.e. T wave amplitude, Q wave amplitude and ST deviation measure; were extracted for each beat and combined for 12-leads forming a 36 dimensional feature vector. These features were used for the MI detection and some localizations purpose.

4.2 Principal Component Analysis

Principal component analysis (PCA) [17] is a mathematical procedure that transforms a number of possibly correlated variables into a smaller number of uncorrelated variables called principal components. It is a dimensionality reduction technique and it finds the components in which the direction of variance is

maximized. PCA was used to generate the second set of features in this research as described in the following sections.

4.2.1 Introduction

Before going to describe PCA we go through some statistical concepts that are necessary for understanding PCA.

4.2.1.1 Standard Deviation and mean

Given a data set or sample population the mean is the sum divided by the number of data point's i.e. for a data set X the mean is calculated to be:

$$\tilde{X} = \sum_i^n Xi \ /n$$

The mean doesn't tell us a lot about the data except for a sort of middle point. For example, these two data sets have exactly the same mean, but are obviously quite different:

$$[20\ 0\ 8\ 12] \text{ and } [11\ 12\ 8\ 9]$$

The difference between the datasets is that the spread of the data is different. The Standard Deviation (SD) of a data set is a measure of how spread out the data is. The way to calculate it is to compute the squares of the distance from each data point to the mean of the set, add them all up, divide by n-1, and take the positive square root. As a formula the standard deviation is:

$$S = \sqrt{\frac{\sum_i^n (Xi - \tilde{X})^2}{n-1}}$$

Where s stands for standard deviation. When calculating the standard deviation for sample population the divide by n-1 is used while when calculate the standard deviation of whole dataset divide by n is used.

4.2.1.2 Variance

Variance is another measure of the spread of data in a data set , almost identical to the standard deviation. The formula is:

$$S^2 = \frac{\sum_i^n (Xi - \tilde{X})^2}{n-1}$$

This is simply the standard deviation squared. Both these measurements are measures of the spread of the data. Standard deviation is the most common measure, but variance is also used.

4.2.1.3 Covariance

Many data sets have more than one dimension, and the aim of the statistical analysis of these data sets is usually to see if there is any relationship between the dimensions. Covariance means how the change in one variable affects the other or how the variables vary relative to each other. It is always measured between two dimensions. If we have three dimensional data (x, y, z) the we can measure the covariance between x and y dimensions, x and z dimensions and so on. The formula for calculating covariance comes from that of variance where we replace one dimension by two different dimensions. The formula for variance in expanded form is:

$$var_X = \frac{\sum_i^n (Xi - \tilde{X})(Xi - \tilde{X})}{n-1}$$

Now when we have two dimensions namely x and y for calculating covariance between x and y we can write the formula:

$$covar(X, Y) = \frac{\sum_i^n (Xi - \tilde{X})(Yi - \tilde{Y})}{n-1}$$

Since multiplication is commutative, it implies that covar(x,y) is same as covar(y,x).

4.2.1.4 The covariance Matrix

Covariance is always measured between 2 dimensions. If we have a data set with more than 2 dimensions, there is more than one covariance measurement that can be

calculated. For a three dimensional data set (x, y, z) we can calculate covar (x, y), covar(x, z), covar(y, z).

All the covariance values across the dimensions are calculated and put in a matrix which is called covariance matrix. For N dimensional dataset the covariance matrix is an NxN matrix. On the main diagonal of the matrix the values are simple variances and since covar(x,y) is same as covar(y,x) so the matrix is symmetric along the main diagonal. For example for a three dimensional dataset (x, y, z) the covariance matrix is :

$$C = \begin{matrix} covar(x,x) & covar(x,y) & covar(x,z) \\ covar(y,x) & covar(y,y) & covar(y,z) \\ covar(z,x) & covar(z,y) & covar(z,z) \end{matrix}$$

So we can see that at the main diagonal, the values are simple variances and the matrix is symmetric along the main diagonal.

4.2.1.5 Eigenvectors and Eigenvalues

Let A be an *nxn* matrix. The eigenvector of *A* is a vector *v* such that:

$$A\boldsymbol{v} = \lambda\boldsymbol{v}$$
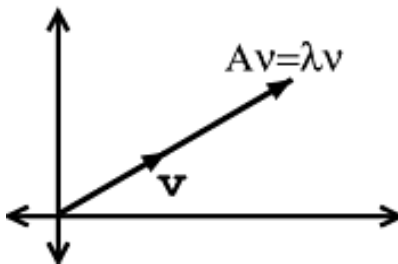
Figure 4.5 Eigenvector and eigenvalue

Where λ is called the corresponding eigenvalue. The vector's length is simply scaled by variable λ. Equation (1) is further manipulated to find the eigenvalues and eigenvectors of a given matrix *A*.

$$Av = \lambda v$$

$$(A - \lambda)v = 0$$

$$(A - \lambda I)v = 0$$

Where *I* is the identity matrix. So *(A-λI)* is just a new matrix. If *(A-λI) v=0* for some **v≠0** then the matrix (A-λI) is not invertible and hence:

det [A-λI] = 0

This determinant turns out to be a polynomial expression and we can solve it for calculating the eigenvalue *λ*. Given an eigenvalue *λi* the associated eigenvectors are given by:

$$Av = \lambda_i v$$

$$A \begin{bmatrix} v_1 \\ v_2 \\ \vdots \\ v_n \end{bmatrix} = \begin{bmatrix} \lambda_1 v_1 \\ \lambda_2 v_2 \\ \vdots \\ \cdot \\ \lambda_n v_n \end{bmatrix}$$

The set of n equations with n unknowns, simply solve the n equations to find the n eigenvectors. Eigenvectors can only be found for square matrices. And, not every square matrix has eigenvectors, and a given NxN matrix, that does have eigenvectors there are N of them for example a 3x3 matrix have three eigenvectors. Another property of eigenvectors is that if even we scale the matrix by some number before multiplying it, we'll get the same eigenvalue/multiple as a result because scaling a vector only changes its length not the direction. Lastly all the eigenvectors of a matrix are perpendicular/at right angles to each other, also called orthogonal. This is important because it means that you can express the data in terms of these perpendicular eigenvectors.

4.2.2 Computation of Principal Components

In this procedure PCA is applied on selected regions such *ST-T* region and *Q* wave region; of the baseline and iso electric level removed ECG signal. The *ST-T* region that was selected comprises of *100* samples (0.5 seconds duration) and *Q* wave region that was selected contains *15* samples (0.06 seconds duration) for each beat in each lead across the database (figure 4.5).
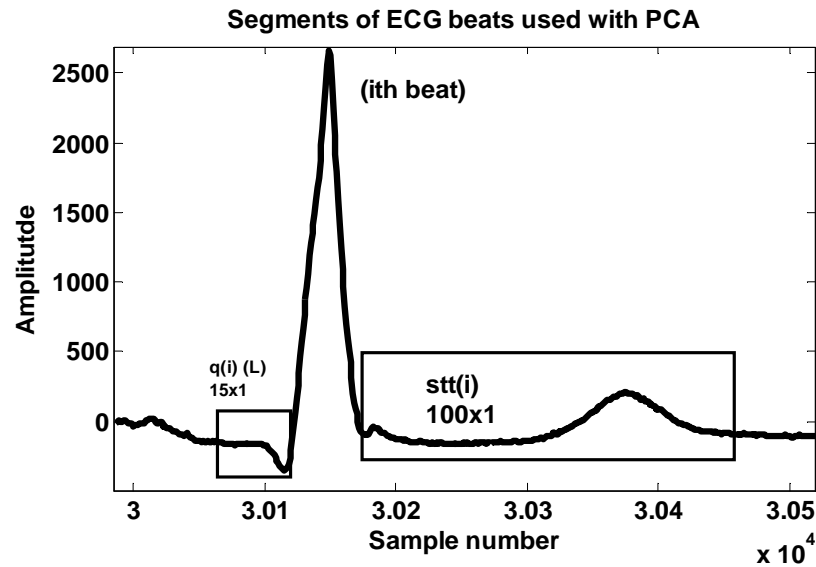
Figure 4.5 Regions of the beat that were selected for PCA to be applied on.

For each lead l two separate matrices $\mathbf{S}_l$ and $\mathbf{Q}_l$ were formed corresponding to *ST-T* region and *Q* wave region by collecting these regions from all the beats and then selecting *3000* beat's regions at random in both cases as follows:

$$\mathbf{S}_l = [\mathbf{stt}_l^1 ... \mathbf{stt}_l^k ... \mathbf{stt}_l^{3000}]_{(100 \times 3000)}$$

$$\mathbf{Q}_l = [\mathbf{q}_l^1 ... \mathbf{q}_l^k ... \mathbf{q}_l^{3000}]_{(15 \times 3000)}$$

Where $\mathbf{stt}_l^k$ is the *ST-T* region corresponding to k^{th} beat in lead l; similarly $\mathbf{q}_l^k$ is the *Q* wave region corresponding to k^{th} beat in lead *l*. After combining, data normalization was performed by normalizing each row *m* of S_l as follows:

$$S_l^m = \frac{S_l^m - \mu_{S_l}^m}{\sigma_{S_l}^m}$$

Where $\mu_{S_l}^m$ is the mean of mth row of $\mathbf{S}_l$ and $\sigma_{S_l}^m$ is the standard deviation of mth row of $\mathbf{S}_l$. Similarly $\mathbf{Q}_l$ was normalized as follows:

$$Q_l^m = \frac{Q_l^m - \mu_{Q_l}^m}{\sigma_{Q_l}^m}$$

The corresponding Eigen vectors matrices for each of S_l and Q_l were generated by PCA as:

$$\mathbf{V}_l^s = [\mathbf{v}_l^{s_1}...\mathbf{v}_l^{s_k}...\mathbf{v}_l^{s_n}]_{100 \times s_n^l}$$

$$\mathbf{V}_l^q = [\mathbf{v}_l^{q_1}...\mathbf{v}_l^{q_k}...\mathbf{v}_l^{q_n}]_{15 \times q_n^l}$$

Where s_n^l and q_n^l are the number of principal components for *ST-T* and *Q* region corresponding to lead l respectively and $\mathbf{V}_l^{s_k}$ is the kth Eigen vector corresponding to lead l with n_s^l and q_l^n are chosen such that 98% variance of the data is captured. Table 4.1 contains a summary of the above parameters for each lead. As shown in the table 4.1 the final feature vector generated by PCA is 117 dimensional much less than 1380 dimensional vector before applying PCA.

Table 4.1 Computation of principal components for each lead

ECG lead	stt_l^i	q_l^i	stt'_l^i	q'_l^i	y^l
I	100	15	12	5	17
II	100	15	9	5	14
III	100	15	8	6	14
AVI	100	15	11	5	16
AVF	100	15	13	5	18
AVR	100	15	8	6	14
V1	100	15	10	4	14
V2	100	15	9	5	14

V3	100	15	8	5	14
V4	100	15	9	5	14
V5	100	15	11	4	15
V6	100	15	10	4	14
For 12 leads	1200	180			*177*

4.2.3 Dimensionality Reduction

After calculating PCA models (as described in previous section), dimensionality reduction of the training and testing data extracted from ST-T and Q wave region was made as follows:

$$stt\,''^{i}_{l} = (V^{s}_{l})^{T}\,stt^{i}_{l}$$

$$q\,''^{i}_{l} = (V^{q}_{l})^{T}\,q^{i}_{l}$$

Where $stt\,''^{i}_{l}$ and $q\,''^{i}_{l}$ are the reduced representation of extracted features stt^{i}_{l} and q^{i}_{l} corresponding to lead l. These reduced feature sets were then combined to have a feature set for each lead l in each patient's record.

$$\mathbf{y}^{i} = \begin{bmatrix} stt\,''^{i}_{l} \\ q\,''^{i}_{l} \end{bmatrix}$$

Combining the 12 leads features forms final input feature matrix for each patient who can be either used for training or testing the classifier.

CHAPTER 5
CLASSIFICATION

Classification is the task of categorizing a given pattern into one of several types/classes. In this work the beat vise classification is carried out on the features extracted (as described in previous chapter) for both detection and localization of MI separately.

5.1 Introduction

The classification task is divided into Detection and Localization of Myocardial Infarction. The number of classes selection is different for detection and localization. In the detection process we treat healthy control/non infarction as one class and all other infracted types as the other class. So the detection is basically a two class classification i.e. classifying infracted subjects vs. non infracted subjects. Detection is performed separately on features from time domain measures as well as feature extracted using PCA approach. For localization we have ten types of myocardial infarction each as different class. Different combinations of the classes are taken as different datasets and performed classification (described later). Back propagation neural networks (BPNN) is used currently in this work as classifier since it has been successfully applied by the researchers for such disease classification tasks [12], [13] and [16]. The complete description BPNN application as classifier is followed in subsequent sections.

5.2 Literature Survey

Several different techniques exists for ECG feature and classification such as back propagation neural nets (BPNN), fuzzy logic based, and hybrid techniques such as neuro fuzzy see [12], [13], [14], [15] and [16]. Every technique has its own advantages and disadvantages but the classifier usage is dependent on the nature of

the classification problem and the nature of input feature matrix. The input feature matrix with more discrimination can be classified easily with reasonable accuracy by most of the classifiers. Some classifiers are biased towards the class with more training examples in the input matrix, so such classifier can perform better only if equal number of training examples is available but it's not usually the case. In disease classification, back propagation neural networks have been widely used. Several researchers have applied BPNN for the detection of MI on their feature sets [12], [14] and [16] and hybrid approach (NN+Fuzzy) for localization [13]. The summary of literature results for detection and localization of MI is given in the table 5.1. See the reference section for authors and paper title.

Reference#	*Results*
12	Sensitivity for detecting Anterior MI=79% , Specificity=97% with time domain QRS measure as features and BPNN as classifier
13	The sensitivity and specificity are 84.6% and 90.0% for the testing set using neuro fuzzy approach
16	The sensitivity of the neural networks was 95% higher than the cardiologist at a specificity of 86.3%

5.3 Detection of MI

In this study myocardial infarction detection was treated as two class classification with infracted and non infracted classes. The input data obtained from feature extraction process was classified using BPNN for detection. Half of the patient's data was used for testing and remaining was used for training and cross validation. The datasets for training, cross validation and testing were kept disjoint. Neural net architecture was optimized using cross validation dataset. The optimum parameters were found to be TrainRP as learning algorithm, two hidden layers with 20 neurons in the first hidden layer and 5 neurons in the second hidden layer. The learning algorithm "TrainRP" in matlab neural net toolbox is memory efficient and can handle large number of training examples such as in this case.

5.4 Localization of MI

Localization was done using both PCA based features as well as time domain features separately with back propagation neural network as classifier. For checking the maximum classification accuracy we used the extracted features of different types of MI combining in six data sets. In each data set, MI types were put in different classes as shown in the table 5.2. The table includes the types of MI that were used in each data set along with feature extraction method. Each data set was further divided into training, cross validation and testing data for classification with BPNN. The datasets for training, cross validation and testing were kept disjoint. Neural net architecture was optimized using cross validation dataset. The training parameters of BPNN have to be tuned to find a more generalized network therefore training in each case was performed multiple times and cross validation errors were noted for each trained network. The network with minimum cross validation error was used for testing. The BPNN training architectures, cross validation and testing are described in next result's sections.

Table 5.4 Datasets used for MI Localization. The combinations are chosen such that relevant types of MI fall within the same class.

Dataset	Features extraction method	MI Types included in the dataset
1.	PCA	ANTERIOR (class$_1$)
		INFERIOR (class$_2$)
		LATERAL (class$_3$)
		POSTERIOR (class$_4$)
2.	PCA	ANTERIOR, ANTERO SEPTAL , ANTERO LATERAL (class$_1$)
		INFERIOR , INFERO LATERAL , INFERO POSTERIOR (class$_2$)

3.	PCA	ANTERIOR , ANTERO SEPTAL , ANTERO LATERAL (class$_1$)
		INFERIOR , INFERO LATERAL , INFERO POSTERIOR , INFERO-POSTERO-LATERAL (class$_2$)
4.	PCA	ANTERIOR (class$_1$)
		ANTERO LATERAL (class$_2$)
		ANTERO SEPTAL (class$_3$)
5.	Time domain features	ANTERIOR , ANTERO SEPTAL , ANTERO LATERAL (class$_1$)
		INFERIOR , INFERO LATERAL , INFERO POSTERIOR , INFERO-POSTERO-LATERAL (class$_2$)
6.	Time domain features	ANTERIOR (class$_1$)
		INFERIOR (class$_2$)
		LATERAL (class$_3$)
		POSTERIOR (class$_4$)

5.5 Classification Results

This section describes the results for detection and localization of MI. The classifier performance was measured in terms of sensitivity, specificity and accuracy. Using the testing output of the NN classifier a confusion matrix was formed, then using confusion matrix these performance parameters were calculated. The format of confusion matrix that was used is given in the table 5.3.

Table 5.3 Format of confusion matrix

Original/Predicted	Infarcted	Non infarcted
Infarcted	True positives (T_P)	False negatives(F_N)
Non infarcted	False positives (F_P)	True negatives(T_N)

Sensitivity (SE) is calculated as follows:

$$SE(\%) = \frac{T_P}{T_P + F_N} \times 100$$

Where *TP, TN, FP,* and FN represent the number of true positives, true negatives, false positives and false negatives respectively. Specificity (SP) is calculated by the equation:

$$SP(\%) = \frac{T_N}{T_N + F_P} \times 100$$

The classification accuracy can be determined by dividing the sum of true measures by the sum of all measures as follows:

$$ACC(\%) = \frac{T_P + T_N}{T_P + F_N + T_N + F_P} \times 100$$

5.5.1 MI Detection results using PCA based features

Several different neural net architectures were applied on the training data to get the optimized trained net for classification of testing data. A separate cross validation dataset was used for cross validation and the corresponding cross validation errors were noted against each architecture. The details are shown by the graph 5.1 and architecture specs are given in the table below (table 5.4).

Table 5.4 BPNN architectures used for training

S.No	Hidden Neurons combinations	Learning algorithm	Learning rate	Goal	CV error
1	[20 10]	TrainRP	0.3	0.01	0.2674
2	[30 20]	TrainRP	0.1	0.01	0.2179
3	[20 5]	TrainRP	0.5	0.01	0.1342
4	[30 15]	TrainRP	0.3	0.01	0.1881
5	[10 5]	TrainRP	0.5	0.01	0.2765
6	[30 20]	TrainRP	0.3	0.01	0.2074
7	[50 25]	TrainRP	0.3	0.01	0.1820
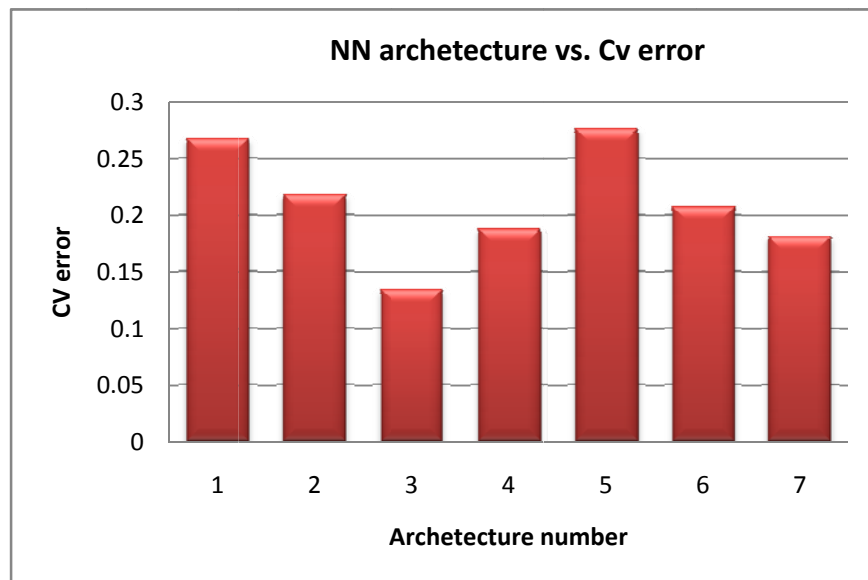
Figure 5.1 Graph showing the cross validation error variation of NN architecture

The confusion matrix given below (table 5.5) presents a summary of the classification results on total of 15686 infarcted type beats and 1610 non infracted type beats. It shows the number of true positives, true negatives and false measures also. The sensitivity, specificity and accuracy have been also calculated.

Table 5.5 MI detection results on PCA

Original/Predicted class	Infarcted class	Non Infarcted class
Infarcted class	14595	1091
Non infracted class	407	1203
Specificity (%)	74.7	
Sensitivity (%)	93.04	
Accuracy (%)	91.34	

5.5.2 MI Detection results using Time Domain Features

In this section, the results obtained by using the time domain features extracted are presented. All the infracted types were placed in class1 and normal were considered as class2. So effectively the detection became a two class classification namely infracted class and non infracted class. In training process several different neural net architectures were applied on the training data to get the optimized trained net for classification of testing data. Cross validation errors were noted against each architecture. The Cross validation error details are shown by the graph 5.2 and architecture specs are given in the table below (table 5.6).

Table 5.6 BPNN architectures applied

S.No	Hidden Neurons	Learning algorithm	Learning rate	Goal
1.	[50 30]	TrainRP	0.3	0.01
2	[15 10]	TrainRP	0.3	0.01
3	[20 5]	TrainRP	0.3	0.01
4	[60 40]	TrainRP	0.3	0.01
5	[50 25]	TrainRP	0.9	0.01
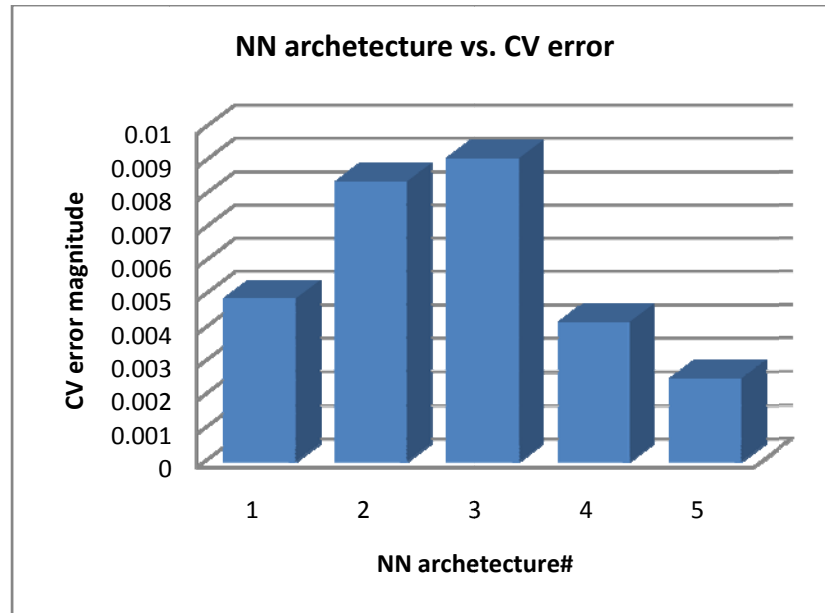
Figure 5.2 Bar graph showing least CV error

In this case the architecture #5 with two hidden layers and [50 25] hidden layer   neuron combination has the least cross validation error as compared to other neural nets that were trained, and has been used to classify the testing data.

5.5.2.1 Results

The confusion matrix given below presents a summary of the classification results. It shows the number of true positives, true negatives and false measures also. The sensitivity, specificity and accuracy have been also calculated.

Number infracted beats used for testing: 10580

Number non infracted beats used for testing: 1840

Table 5.7 Detection results using time domain features

Original/Predicted class	Infracted	Non Infarcted
Infarcted	10316	264
Non Infarcted	16	1824
Sensitivity (%)	97.5	
Specificity (%)	99.1	
Accuracy (%)	97.75	

5.5.2.2 Discussion

The confusion matrix shows that the detection results using time domain features are better as compared to that on PCA. Time domain feature have better discrimination between infracted and non infracted classes. The comparison of results is shown in the figure 5.3.
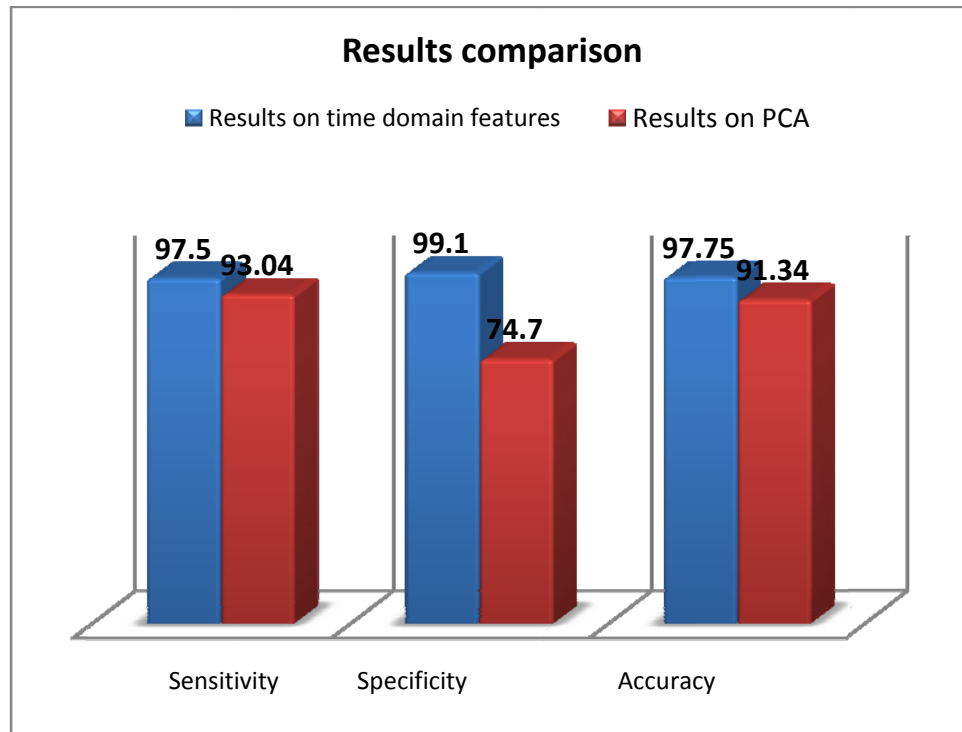
Figure 5.3 Results comparison, Time domain features vs. PCA based for MI detection

5.5.3 MI Localization results using PCA based features

For MI localization purpose, the features extracted from PTB database for each type of MI, were divided into four datasets as mentioned in the table 5.4 above. For each data set, classification was performed separately and results were noted. Several different neural net architectures were applied on the training data to get the optimized trained net for classification of testing data. A separate cross validation dataset was used for cross validation and the corresponding CV errors were noted against each architecture. Some of the parameters remain the same like learning algorithm, number of epochs and goal. Different combinations of the

number of hidden layer neurons were tried. The minimum cross validation error network was used for testing.

5.5.3.1 Results on D*ataset 1*

This dataset contains four different types of MI, that is, anterior, inferior, lateral and posterior infarct as four classes and were classified using BPNN as classifier. The BPNN architecture and corresponding CV error are given in the table 5.8. The architecture*#4* has the least CV error and was used for testing.

Table 5.8 Trained NN architectures and CV errors

S.No	Hidden Neurons	Learning algorithm	Learning rate	Goal	CV error
1.	[12 5]	TrainRP	0.4	0.01	0.0061
2	[20 10]	TrainRP	0.1	0.01	0.0099
3	[30 20]	TrainRP	0.5	0.01	0.0076
4	[30 15]	TrainRP	0.3	0.01	0.0030
5	[50 30]	TrainRP	0.3	0.01	0.0061

The confusion matrix (table 5.9) given below, presents a summary of the classification results. It shows the number of true positives, true negatives and false measures. The sensitivity, specificity and accuracy have been also calculated.

Table 5.9 Classification results using PCA on four types of MI

Original /predicted class	Anterior	Inferior	Lateral	Posterior	SE (%)
Anterior	1640	13	3	194	88.64
Inferior	426	3345	76	144	83.81
Lateral	25	4	153	80	58.33
Posterior	2	1	20	244	91.33
SP (%)	78.35	60.24	60.71	92.40	**Acc=84.52%**

5.5.3.2 Results on *Dataset 2*

In this dataset six MI types have been taken and divided into two classes. Each class contains three related types, that is, *class1* contains anterior, antero septal and antero lateral. *Class2* contains inferior, infero lateral and infero posterior MI. The NN architecture and CV errors are given in the table 5.10 below.

Table 5.10 Trained NN architectures and CV errors using dataset2

S/no	Hidden Neurons	Learning algorithm	Learning rate	Goal	CV error
1.	[15 10]	TrainRP	0.3	0.01	0.0136
2	[15 5]	TrainRP	0.3	0.01	0.0157
3	[20 10]	TrainRP	0.1	0.01	0.0212
4	[30 15]	TrainRP	0.5	0.01	0.0085
5	[20 15]	TrainRP	0.3	0.01	0.0123

On the architecture number four in the table above the cross validation error is less as compared to other neural nets that were trained. It has been used to classify the testing data. The classification results are given by the confusion matrix (table 5.11) below.

Table 5.11 Classification results using dataset2

Original/Predicted	Class1	Class2	SE (%)
Class1	7997	486	
Class2	405	5344	94.27
Specificity (%)	92.95		Accuracy=93.72%

5.5.3.3 Results on *Dataset3*

In this case we have divided the myocardial infarction types into two classes. *Class1* contains anterior, antero-septal and antero-lateral. *Class2* composed of inferior types i.e. inferior, infero lateral, infero -posterior and inferio–postero-lateral MI. The NN architecture and CV errors are given in the table 5.12 below. The network with minimum cross validation error was selected for testing.

Table 5.12 NN architectures and CV errors

S/no	*Hidden Neurons*	*Learning algorithm*	*Learning rate*	*CV error*	*Goal*
1.	[15 5]	TrainRP	0.3	0.0317	0.01
2	[20 10]	TrainRP	0.3	0.0761	0.01
3	[30 15]	TrainRP	0.5	0.0905	0.01
4	[50 20]	TrainRP	0.3	0.0494	0.01
5	[50 30]	TrainRP	0.3	0.1312	0.01
6	[50 40]	TrainRP	0.3	0.0663	0.01

The confusion matrix (table 5.13) given below presents a summary of the classification results. It shows the number of true positives, true negatives and false measures also. The sensitivity, specificity and accuracy have been also calculated.

Table 5.13 Classification results on dataset4

Original/Predicted class	class1	class2	SE (%)
class1	8430	683	
class2	340	6881	92.5
SP (%)	95.29		Accuracy (%) = 93.73

5.5.3.4 Results on *Dataset4*

In this case we have three anterior infarction types. We have taken anterior as *class1*, antero lateral as *class2* and antero septal as *class3*. The feature set used is that extracted using PCA. This classification shows that to what extent PCA feature extraction plus neural net as classifier can classify/discriminate between anterior types of infarctions themselves. Cross validation errors were noted against each architecture and the neural net with minimum cross validation error was selected for testing.

Table 5.14 NN architecture and CV errors

S/no	Hidden Neurons	Learning algorithm	Learning rate	Goal	CV error
1.	[30 20]	TrainRP	0.1	0.01	0.8958
2	[40 25]	TrainRP	0.3	0.01	0.9906
3	[60 50]	TrainRP	0.5	0.01	0.9029
4	[60 30]	TrainRP	0.5	0.01	0.4953
5	[50 25]	TrainRP	0.3	0.01	0.9721

The confusion matrix (table 5.15) given below, presents a summary of the classification results. It shows the number of true positives, true negatives and false measures also. The sensitivity, specificity and accuracy have been also calculated for each class.

Table 5.15 Classification results on dataset4

Original/predicted class	Anterior	Antero lateral	Antero septal	Sensitivity%
Anterior	1401	176	270	75.8
Antero lateral	639	1032	226	54.4
Antero septal	719	432	3559	75.56
Specificity (%)	50.7	62.92	87.76	
Accuracy (%) = 70.87				

5.5.4 MI localization results using Time Domain Features

The extracted time domain features from PTB database were also used for MI localization for comparison with PCA based technique. In this case we formed two data sets as shown in the table 5.4. Classification was performed on each data set separately and results were noted.

5.5.4.1 Results on *Dataset1*

In this *dataset* the MI types were divided into two classes. *Class1* contains anterior, antero septal and antero lateral MI types. *Class2* composed of inferior types i.e. inferior, infero lateral, infero posterior and inferio postero lateral. The classification was done using BPNN was classifier. Several different NN architectures were applied and CV errors were noted as shown in the table 5.16 below.

Table 5.16 CV error for each NN architecture

S/no	Hidden Neurons	Learning algorithm	Learning rate	Goal	CV error
1.	[15 10]	TrainRP	0.3	0.01	0.8958
2	[30 15]	TrainRP	0.3	0.01	0.3734
3	[50 25]	TrainRP	0.3	0.01	0.3984
4	[40 30]	TrainRP	0.3	0.01	0.3891

The results are given by the confusion matrix below along with other parameters.

Table 5.17 Classification results

Original/predicted	Class1	Class2	Specificity (%)	Sensitivity (%)
Class1	1481	599	90.44	71.2
Class2	107	1013		
Accuracy (%)	77.93			

5.5.4.1 Results on *Dataset2*

In this dataset, the time domain features of MI types included are Anterior, Inferior, Lateral and Posterior. Each type of MI has been labeled as separate class as shown in the table 5.4 previously. The classification was done using BPNN classifier. The CV errors were noted on each architectures and testing was done on the neural net with minimum CV error. The classification results are give in the table 5.18 as follows:

Table 5.18 Classification Results

Class	*Sensitivity*	*Specificity*
Anterior	62.0	69.9
Inferior	47.1	61.2
Lateral	81.1	51.2
Posterior	98.1	54.4

5.5.5 Discussion

The time domain features with neural networks classifies infracted and none infracted (myocardial infarction detection) with best performance parameters i.e. Sensitivity, specificity and accuracy as compared to that of PCA based features (The results comparison is shown in figure 5.3).

The performance of time domain features is not good on localization because time domain features does discriminate in case of infracted vs. non infracted but overlaps in case when we try to classify within infracted classes themselves. For example to classify anterior infarction vs. inferior infarction, time domain features overlap and can't classify correctly. On the other hand, the feature extraction using PCA have good results on localization as shown by the localization results. A comparison of the classification results is shown on time domain features and PCA with datasets that has the same MI types combinations in figure 5.4 and 5.5. The better results on PCA are due to the reason that features extracted using PCA are

more discriminating within infracted classes. It has very interesting results when try to classify quite different types of infarcts such as anterior types vs. inferior types of infarction.
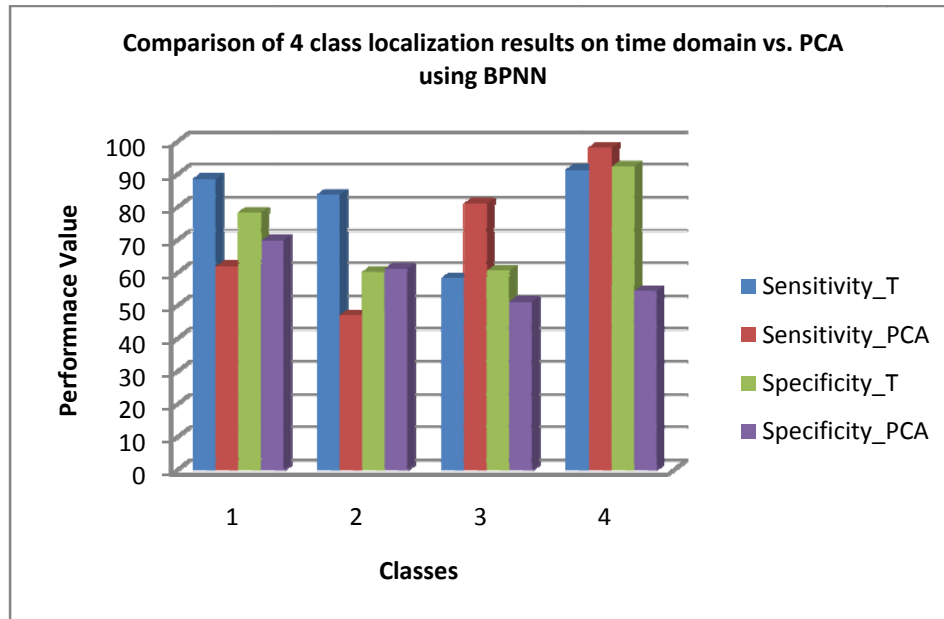
Figure 5.4 Results comparison on dataset1 of PCA vs. Dataset2 of Time domain features
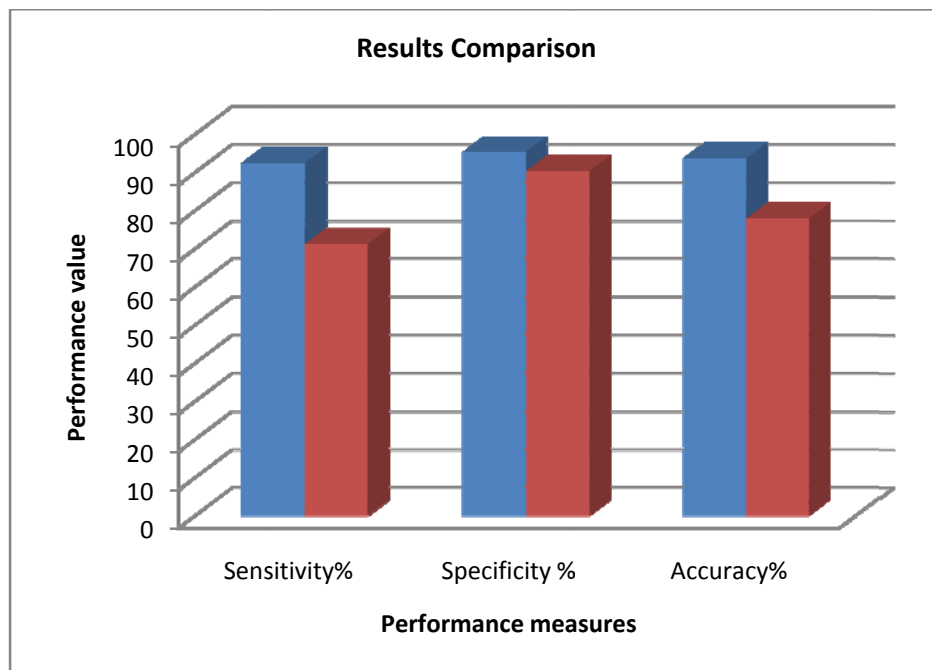
Figure 5.5 Results Comparison of dataset3 of PCA and dataset1 of time domain features

Finally we noted from the results that PCA also does have a problem when try to classify similar category of infarcts i.e. infarcts which have some common main artery involved. For example in anterior types of infarctions such as anterior, antero lateral and antero septal, PCA have poor results. The reason is again features overlapping. There is a need for some new or hybrid type of feature extraction and classification techniques such as neuro fuzzy, which may improve localizing such similar kind of infarcts.

CHAPTER 6
CONCLUSION AND FUTURE WORK

This work was aimed at the ECG based automatic detection and localization of myocardial infarction as a decision support system for cardiac expert with main focus on implementing features extraction and classification techniques. We started from taking raw ECG from PTB database, performing signal pre processing such as baseline removal, QRS delineation and iso electric level detection. The main focal work started from feature extraction. We considered three regions of ECG beat for feature extraction, that is, ST level, Q wave and T wave region. Time domain features were extracted using these regions such as T wave amplitude, Q wave amplitude and ST deviation. This was the first feature (36 dimensional) set to be classified for detection and localization purpose. The second type of feature extraction set (117 dimensional) was obtained by applying PCA on those MI specific regions. Detection and localization was done using BPNN as classifier. The detection results on time domain features came out to be better than that of PCA, that is, the time domain features can discriminate well between infarcted vs. non infarcted type. For localization, PCA based features performed better than time domain features. However the current PCA based features with BPNN classifier performed poor on more than *4* class localization. The future work in this direction is to work on hybrid feature extraction and classification algorithms such as neuro fuzzy to improve the multi class localization performance.

CHAPTER 7
REFERENCES

[1]   PhysioBank, URL**:** www.physionet.org.

[2]   K. Daqourq, "ECG baseline wanders reduction using DWT", Asian journal of information technology 4(11): 989-995, 2005.

[3]   Afsar Minhas, F.A. and M. Arif, "QRS Detection and Delineation Techniques for ECG Based Robust Clinical Decision Support System Design", in National Science Conference. 2007: Lahore, Pakistan.

[4]   MA. Mneimneh, EE. Yaz, MT. Johnson and RJ. Povinelli, "An Adaptive Kalman Filter for Removing Baseline Wandering in ECG Signals", Marquette University, Milwaukee, WI, USA.

[5]   Leif Sornmo and Pablo Laguna, Bio electrical signal processing in cardiac and neurological applications, ELSVIER academic press.

[6]   Gari D.Clifford, Advanced methods and tools for ECG data analysis, Artech-House INC, 2006.

[7]   ECGpedia, URL**:** www.ECGpedia.org.

[8]   Mattias Ohlsson et al, "Acute Myocardial Infarction: Analysis of the ECG using ANN".

[9]   Bo Hedén, MD, PhD et al. "Acute Myocardial Infarction Detected in the 12-Lead ECG by Artificial Neural Networks", American Heart Association, Inc, 1997.

[10]   "Myocardial Ischemia, Injury and Infarction", American Heart Association, URL: http://www.americanheart.org.

[11]   Martinez, J.P., et al., "A wavelet-based ECG delineator: evaluation on standard databases", Biomedical Engineering, IEEE Transactions on, 2004. 51(4): p. 570-581.

[12]   Reddy MRSE, L. Svensson, J. Haisty and W.K. Pahlm, "Neural network versus electrocardiographer and conventional computer criteria in diagnosing anterior

infarct from the ECG", In Computers in Cardiology; 11-14 Oct.1992. 1992: 667 - 670.

[13]   HL Lu KO, P Chia, "An Automated ECG Classification System Based on a Neuro-Fuzzy System**,** In *Computers in Cardiology*. 2000: 387-390.

[14]   MA Mneimneh and RJ Povinelli, "RPS/GMM Approach toward the Localization of Myocardial Infarction", Marquette University, WI, USA.

[15]   Timmis AD, "Early diagnosis of acute myocardial infarction", BMJ. 1990; 301:941-942.

[16]   Bo Heden, Hans Ohlin, Ralf Rittner and Lars Edenbrandt, "Acute Myocardial Infarction Detected in the 12-Lead ECG by Artificial Neural Networks."

[17]   Lindsay I Smith, "Principal Components Analysis", February 26, 2002.